Doping of Carbon Nanotubes

Chapter for inclusion in forthcoming book
"Doped Nanomaterials and Nanodevices", Ed. Wei Chen (2007).

Marianne Glerup

Department of Chemistry, University of Oslo, PO Box 1033, 0315 Oslo, Norway.

Mail : marianne.glerup@kjemi.uio.no, Tel *:+47 228 55676 Fax : +47 228 55441*

Vojislav Krstić

Centre for Research on Adaptive Nanostructures and Nanodevices, Trinity College Dublin, Dublin 2, Ireland

Mail : krsticv@tcd.ie, Tel : +353-1-896 3026, Fax : +353-1-896 3037

Chris Ewels

Institute des Materiaux, UMR6502 CNRS-Université de Nantes, 2 rue de la Houssinière, B. P. 32229, 44322 Nantes, France.

Mail : chris@ewels.info*, Tel :+33 2 40 37 64 07, Fax : +33 2 40 37 39 91, Web: www.ewels.info*

Michael Holzinger

Laboratoire d'Electrochimie Organique et de Photochimie Rédox (CNRS UMR 5630) Institut de Chimie Moléculaire de Grenoble (FR CNRS 2607), Université Joseph Fourier, BP 53, 38041 Grenoble Cedex 9, France.

Mail: michael.holzinger@ujf-grenoble.fr, Tel: +33 4 76 51 44 03, Fax: + 33 4 76 51 49 98

Gregory Van Lier

Free University of Brussels (VUB), General Chemistry (ALGC), Pleinlaan 2, B-1050 Brussels, Belgium.

Mail : gvanlier@nanoscience.be*, Tel :+32 2 629 35 16, Fax : +32 2 629 33 17*

Contents

1. Introduction

Since their discovery in 1991, carbon nanotubes (CNTs) have intrigued and inspired physicists, chemists, biologists and recently medical scientists in their research. This interest in CNTs, consisting in its simplest form of a single, seamlessly wrapped graphene sheet, is based on their extraordinary properties. These stem from two basic features characterising a carbon nanotube: (i) a nano-sized structure with a very high aspect-ratio and a delocalised electron system, and (ii) an all-carbon, all-surface molecular structure.

The first point is responsible for the outstanding electronic and thermal properties of CNTs. The high aspect-ratio of this nano-sized tubular structure leads to strong confinement effects. These result in a pronounced one-dimensional character of the electron system and the phonon spectrum of a CNT. Due to this one-dimensional character the interaction between electrons and phonons is very weak. As a consequence, charge transport is ballistic in CNTs at room-temperature and very high thermal conductivities[1,2] (a few 10^3 W/Km) close to that of diamond (highest thermal conductivity known) are achieved. Notably, the cylindrical symmetry together with the delocalised electron system makes CNTs rather insensitive to lattice defects.

Based on these properties, CNTs are nowadays of high interest as a model for one-dimensional systems in fundamental research and are also under active development as field effect transistors[3, 4, 5], diodes, gigahertz oscillators[4], interconnects in integrated circuits, logic gates[3,4,5] and novel non-volatile memory devices[6].

The second point – being an all-carbon, all-surface molecular structure – is responsible for the high interest of chemists, biologists and medical scientists in CNTs. The (bio-)chemistry of carbon is probably one of the most intensively studied research

fields, simply because of the extremely high abundance of carbon-based materials in our natural environment. Being an all-carbon molecular structure in combination with a (relatively) large surface accessible for chemical treatment, CNTs represent excellent starting points and building blocks of a novel class of bottom-up created materials. These properties of CNTs have led to studies on their application as gas-[7,8,9] and bio-sensors[10], drug transducers and gene delivery vehicles on the cellular level[11],[12] and ion channel blockers[13].

Since the electronic properties of CNTs are strongly connected to the delocalised electron system, obviously any (chemical) modification of the CNTs will influence these properties. Consequently, by the proper choice of the type of modification the electronic properties of a CNT can be deliberately tuned. The tuning of the electronic properties is also referred to as "doping" the CNT.

In this chapter we review the field of carbon nanotube doping, in particular emphasising where this differs significantly from doping of bulk semiconductor materials.

We start with an introduction to carbon nanotubes (CNTs) in general and their electronic structure and transport properties. In Section 3 we discuss some of the challenges and solutions specific to carbon nanotube use in electronics. We then discuss the variety of possible approaches to modify the electronic properties of carbon nanotubes in Section 4. In particular nanotube functionalisation is covered in Section 4.1, taking nanotube fluorination as a specific in-depth example in Section 4.4. Finally in Section 5 we discuss in more detail the transport behaviour of carbon

nanotubes and doped nanotube systems, before drawing some general conclusions in Section 6.

2. Electronic properties of Carbon nanotubes

There are many reviews, indeed whole textbooks, written on carbon nanotubes, and for more in-depth coverage than we can provide here we recommend the reader to try[14,15,16].

CNTs are a tubular form of carbon with exceptionally high aspect ratio, located structurally between planar graphene/graphite layers and molecular fullerenes. Their electrical properties have initiated a tremendous number of theoretical and experimental studies. This has been supported by progress in (sub-)micro-fabrication processes of metals and semiconductors which opened the way to electrical contacting of single molecules or a relatively small number of molecules. This and the potential use of CNTs for organic based integrated circuits as conducting wires on a molecular scale, as an electrically active element itself, as well as an almost perfect model system for fundamental research reflects the fascination of this molecular based structure.

A single walled carbon nanotube (SWNT) is structurally equivalent to a sheet of graphene rolled into a tube (see Figure 1a), i.e. each carbon atom has three neighbours, lying in the plane of the tube wall in a hexagonal arrangement. Such an arrangement minimises the number of carbon dangling bonds since it has no edge sites compared

to an equivalent graphene sheet; energetically offset against this is the out-of-plane distortion caused by the curvature of the tube wall.

Multi-walled nanotubes (MWNTs) consist of multiple tubes arranged coaxially, with typical inter-wall spacing of 0.34-0.36 nm reminiscent of turbostratic graphite (see Figure 1b).   In principle MWNTs span the whole gamut from double walled nanotubes (DWNTs) - having diameters close to those of SWNTs - up to macroscopic carbon fibres, which have been shown to sometimes feature nanotubes at their cores. Obviously a material spanning such a wide range of dimensions from nano- to micro-scopic can have a similarly varying range of properties.   What is commonly referred to as a MWNT typically has a diameter an order of magnitude greater than that of SWNTs, with number of concentric walls varying from two up to hundreds.

(a)

(b)

(e)

(d)
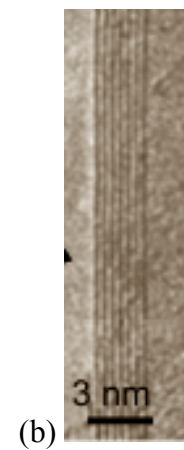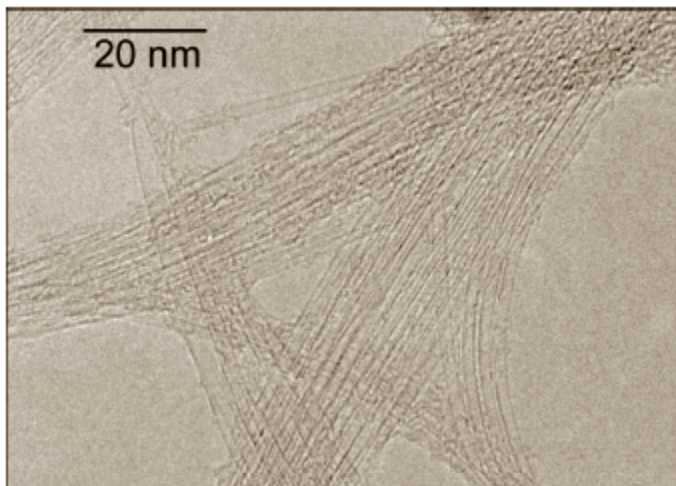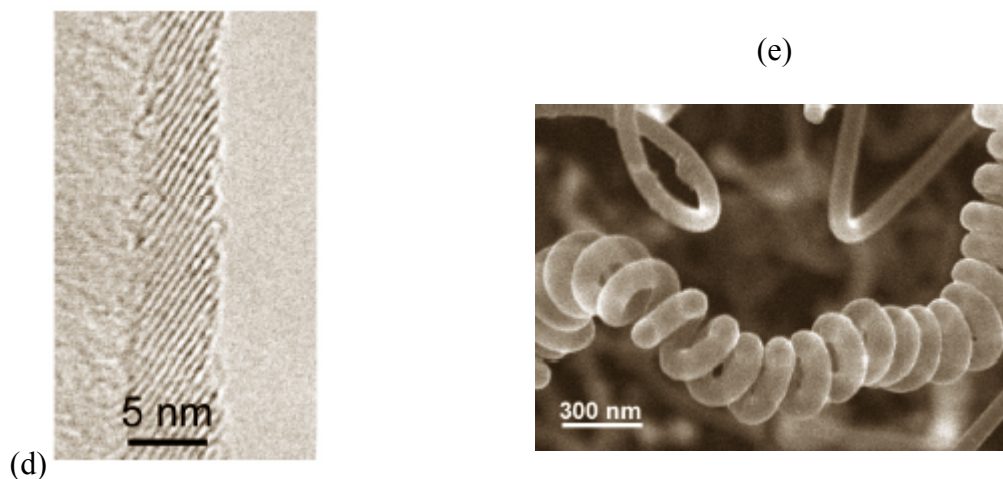
Figure 1. Different members of the carbon nanotube family. (a) Single walled nanotubes arranged in bundles (SWNT), (b) Multi-walled nanotube (MWNT) tube wall (c) Herringbone nanotube wall (d) spiral tube.

As well as cylindrical structures, a variety of other more complex tubular nanometric carbon structures are known to form. These notably including those with herringbone cross section (similar to a stack of cones, see Figure 1c), spiral tubes (similar to a telephone cord, see Figure 1d) and tubes with internal partition walls (these last two are discussed in more detail below).

Inter-tube interaction is strong (for SWNTs this is quoted as ranging from 0.5[17] to 0.95 eV/nm[18]) and thus tubes are commonly observed in hexagonally packed bundles. Various techniques are used to debundle and/or isolate individual tubes, typically using surfactants and/or sonication. Although the inter-tube interaction is often claimed to be of a van der Waals type, it is likely that it is simply weak long-range covalent bonding (interlayer interaction in graphite, often ascribed to van der Waals forces, can in fact be accurately modelled using density functional techniques which do not include any van der Waals type interactions[19,20]).

SWNTs have diameters typically in the range 0.9 to 2 nm, and lengths varying from a few hundred nanometres up to 4 cm or more[21]. They can be semi-metallic (often referred as metallic), or semiconducting depending on their structure.

2.1 Physical structure of carbon nanotubes

A carbon nanotube can be obtained by rolling up the graphene sheet seamlessly along a certain direction. For this it is of importance to define at least two lattice sites which have to be brought into overlap. All others are then determined due to the six-fold symmetry of the graphene lattice and by the condition that a CNT has a cylindrical configuration. These two points can be connected by the chiral vector

$$\vec{C}_{n,m} = n\vec{\alpha}_1 + m\vec{\alpha}_2$$

which is just a linear combination of $\vec{\alpha}_1$ and $\vec{\alpha}_2$ where $n,\ m$ are integers. The symmetry of the graphite lattice is such that chiral vectors where $m>n$ have symmetric equivalents with $m<n$, so the condition is imposed that $m \geq n$. Thus a particular SWNT can be defined using a pair of integer indices (n,m), which together define the chiral vector of the nanotube (Figure 2).

This result comes from the two-dimensional graphene-sheet model[22], where a CNT is described by a planar graphene sheet with periodic boundary conditions that take the translational symmetry along the circumference into account. Although this model suffers from a neglect of curvature effects, it provides the main features of the CNTs.

The line along $\vec{C}_{n,m}$ defines the direction in which the graphene sheet has been wrapped, in such a way that the two points which are connected by $\vec{C}_{n,m}$ are overlapping. Consequently, the length of the chiral vector defines the circumference $2\pi r_t$ of the CNT where r_t is the CNT radius, giving the tube diameter as

$$d_t = \frac{\left|\vec{C}_{n,m}\right|}{\pi} = \frac{\sqrt{3}a_{C-C}}{\pi}\sqrt{m^2 + mn + n^2} \; .$$

Due to the sixfold symmetry of the graphene lattice, all possible structures can be classified by three general configurations: armchair CNTs, for which $n = m$, zigzag CNTs that have $n = 0$ and all other CNTs which are referred to as chiral (see Figure **3**). This use of the term chiral is to some extent misleading (indeed, helical is more appropriate). Often armchair and zig-zag nanotubes are also called chiral, although their mirror images are identical to the original.

Figure 2 shows a graphene sheet in which the real-space unit lattice vectors $\vec{\alpha}_1$, $\vec{\alpha}_2$, the so-called chiral vector $\vec{C}_{n,m}$ and the wrapping angle θ are illustrated. The vectors $\vec{\alpha}_1$ and $\vec{\alpha}_2$ have the same length $\sqrt{3}a_{C-C} \approx 2.461\text{Å}$ where a_{c-c} is the distance between second neighbour carbon atoms.
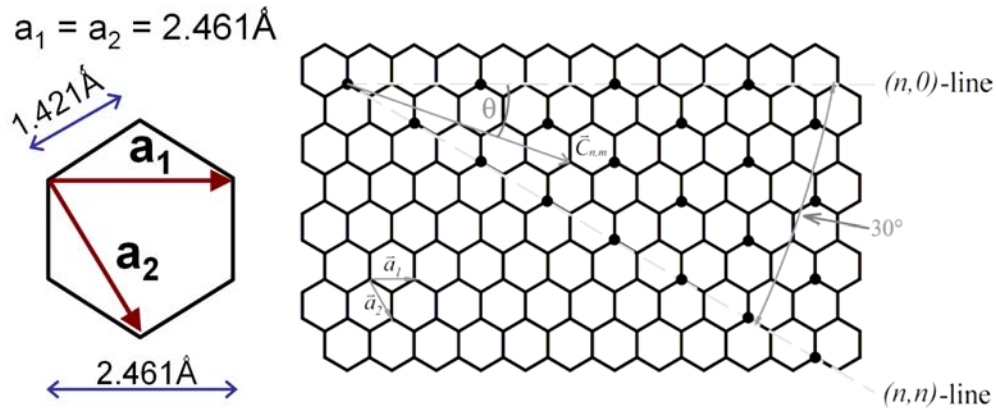
Figure 2. Graphene sheet showing the sixfold-symmetry. Shown are the unit lattice vectors $\vec{\alpha}_1$, $\vec{\alpha}_2$, a chiral vector $\vec{C}_{n,m}$ corresponding to the pair of indices (4,2), the chiral angle θ and the (n,0)- and the (n,n)- line. Due to the sixfold-symmetry of the honeycomb lattice, any θ > 30° can be mapped back on a θ between 0° and 30°, i.e., these CNTs are identical. The black dots denote chiral vectors corresponding to metallic CNTs.

Different wrapping angles lead to a variety of potential nanotube helicities. These can be either left- or right-handed depending on the direction of rolling of the graphene

sheet. The electronic system of CNTs exhibits strong 1D-character, as the absolute values of diameter and length (nm and μm, respectively) give rise to quantum size effects.

Figure 3. The three types of CNTs are shown [23]. The tube to the left is a so-called armchair (n = m), the two tubes in the middle are chiral (n ≠ m,), and the one to the right is a zigzag tube (m = 0). The particular values of the pair of indices (n,m) is addressed to each tube. The description 'armchair' and 'zigzag' come from the circumferential arrangement of carbon atoms.

2.2   Electronic structure of carbon nanotubes

The electronic properties of the graphene sheet (and thus of the CNTs) are mainly determined by the π-electrons since the electrons in the sp^2-hybridised orbitals are strongly localized. In particular, the interaction between the p_z-orbitals leads to (i) the delocalization of the π-electrons and (ii) the formation of bonding π-bands and antibonding $\pi*$-bands.

For CNTs, periodic boundary conditions are introduced to the planar two-dimensional graphene-sheet model due to the translational symmetry around the circumference of

the CNT. To discuss this further it is convenient to shift to reciprocal space. The reciprocal lattice of a graphene layer is again a honeycomb-lattice. A three-dimensional graph of the energy dispersion of graphene of the two lowest subbands in the first Brillouin zone (BZ) is given in Figure 4a derived by tight binding calculations[16]. The six points denoted by K at the edge of the BZ are the only points where the π- and π^*-band touch, and are the reason graphene is a semi-metal. Seen in projection this gives a hexagonal reduced BZ with the K-points located at the hexagonal corners (Figure 4b).
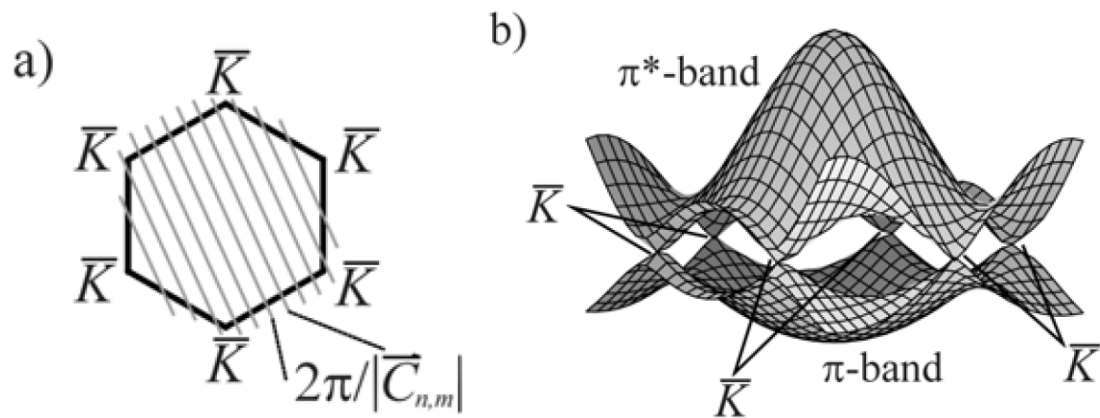
Figure 4. a) Reduced Brillouin zone (BZ) scheme of the graphene. The lines denote allowed k-states for a CNT with diameter $\left|\vec{C}_{n,m}\right|/\pi$. At the K-points, the π- and π^*-band touch. b) 3D-plot of the dispersion relation of the π- and π^*-band from a tight-binding calculation.

If we now compare this with the CNT, we can see that the two dimensional graphene case collapses to 1D for the nanotube. This is because the periodicity around the tube circumference removes dispersion orthogonal to the tube axis, i.e. the kinetic energy around the circumference is quantised. The 2D projection of the reduced BZ for graphene reduces to a series of 1D lines, whose spacing is determined by the circumference of the nanotube, and who orientation is determined by the orientation of the chiral vector (n,m). This is shown in Figure 4a. Thus a CNT band structure is a

slice through the graphene sheet energy-band structure (without periodic boundary conditions) along a certain direction.

It is then clear that the band gap of the nanotube will be determined by the position of these lines on the 2D graphene BZ. Slices which cross the K-points are describing metallic CNTs, as at these points the π- and π*-energy band touch. This in turn leads to a finite density of states (DOS) at the Fermi energy E_F. Other directions correspond to CNTs with a vanishing DOS at E_F, resulting in an energy-gap of typically less than 1 eV. These CNTs are therefore semiconducting.

The information whether a CNT is metallic or semiconducting can be again extracted from the integers (n,m) that classify each CNT, as described above. The pair of indices (n,m) defines the basic electronic character of the nanotube; if *n=m* and if *n-m=3i* (where *i*=integer, i≠0) the tube is semi-metallic, and otherwise it is semiconducting. All armchair tubes are metallic whereas zigzag and chiral nanotubes can exist as either metallic or semiconducting molecular structures.

The 1D electronic nature of a CNT has implications for the electronic density of states (DOS). Consider for simplicity, a one-dimensional free electron gas confined to the length, L, with infinitely high potential walls. The energy eigenvalues are given by $E_v=(\hbar^2/2m)k_v^2$ with *m* the effective mass of the electrons, $\hbar$ the reduced Planck's constant and $k_v = (2\pi/L)v$ the corresponding wave-vector (*v* an integer). The DOS *D(E)* of the system is then simply given by $D(E) = \sum_V \delta(E - E_v)$ where δ denotes the delta-distribution. In the limit of a very large system where the number of energy

eigenvalues is large and the energy difference between adjacent energies E_v is small, *D(E)* can be written as

$$D(E) = \frac{dN}{dE} = \frac{\sqrt{2m}L}{\pi\hbar} E^{-1/2}$$

where *dN* is the number of energy states in the energy interval *dE*. A factor of two for the spin-degeneracy has been considered in the calculation. The DOS shows a divergence as the energy E approaches zero which is known as a *van-Hove singularity*. The $E^{-1/2}$-dependence in the DOS of CNTs can be confirmed in bandstructure calculations[16] and experimentally with the aid of scanning tunnelling microscopy.

a)

b)
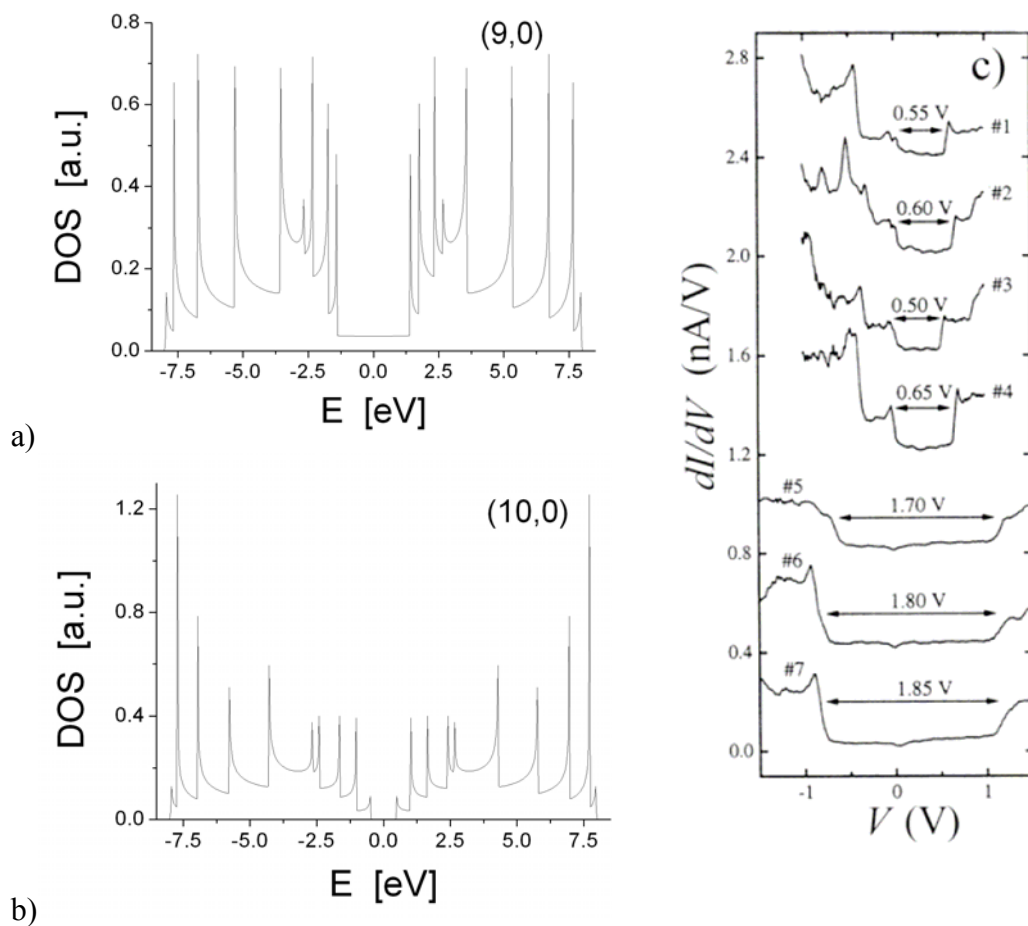
Figure 5. a) Calculated DOS of a (9,0) CNT. At the Fermi energy (here set to zero) a finite density of states exists indicating that the CNT is metallic. b) DOS of a semiconducting (10,0) CNT with vanishing density of states at the Fermi energy. Note that the energy difference between van-Hove-singularities is smaller than for the metallic CNT.
Images kindly provided by Dr Mauro Ferreira, Trinity College Dublin.
c) Derivative dI/dV of the tunnelling current, which is proportional to the density of states, taken from the STM[24]. CNTs #1-#4 are semiconducting, whereas the others are metallic. Van-Hove singularities are apparent, confirming theory. Figure (c) Adapted by permission from Macmillan

In Figure 5a+b, the theoretically calculated DOS of a metallic (9,0) and a semiconducting (10,0) tube, respectively, is shown[16]. Several van-Hove-singularities are visible, each of them corresponding to a certain sub-band of the CNT. In Figure 5c experimental spectroscopy data taken by the scanning tunneling microscope (STM) at room temperature are depicted[24]. The figures show the differential conductance dI/dV for several SWNTs plotted versus the applied voltage V between STM tip and the CNT under investigation. The differential conductance reflects the (local) DOS of the CNT as the tunneling current I is proportional to $\int_{E_F}^{E_F+eV} D_S(E)D_{tip}(E-eV)dE$ where $D_s(E)$ and $D_{tip}(E-eV)$ are the DOS of the sample at the STM tip position and the tip, respectively[25]. Therefore, the derivative of I with respect to V yields $dI/dV \sim D_s(E_F + eV)$. Singularities can be seen in the experimental data confirming the theoretical predictions.

Since all of the above discussion of the electronic properties of isolated SWNTs is based around a graphene model, we would expect deviations from this due to the effects of curvature on the bonding in the nanotube. For example, C-C bond-lengths become slightly polarised; axially oriented bonds shorten and circumferential bonds elongate by a few fractions of a % depending on curvature, as curvature weakens the non-axial π–bonding and consequent aromaticity. This may have a weak effect on conduction pathways and bond site reactivity.

A good summary a 'Periodic Table' of different nanotube properties is shown in Figure 6, showing the relationship between the *(n,m)* indices and other nanotube properties such as diameter, chiral angle and band gap.
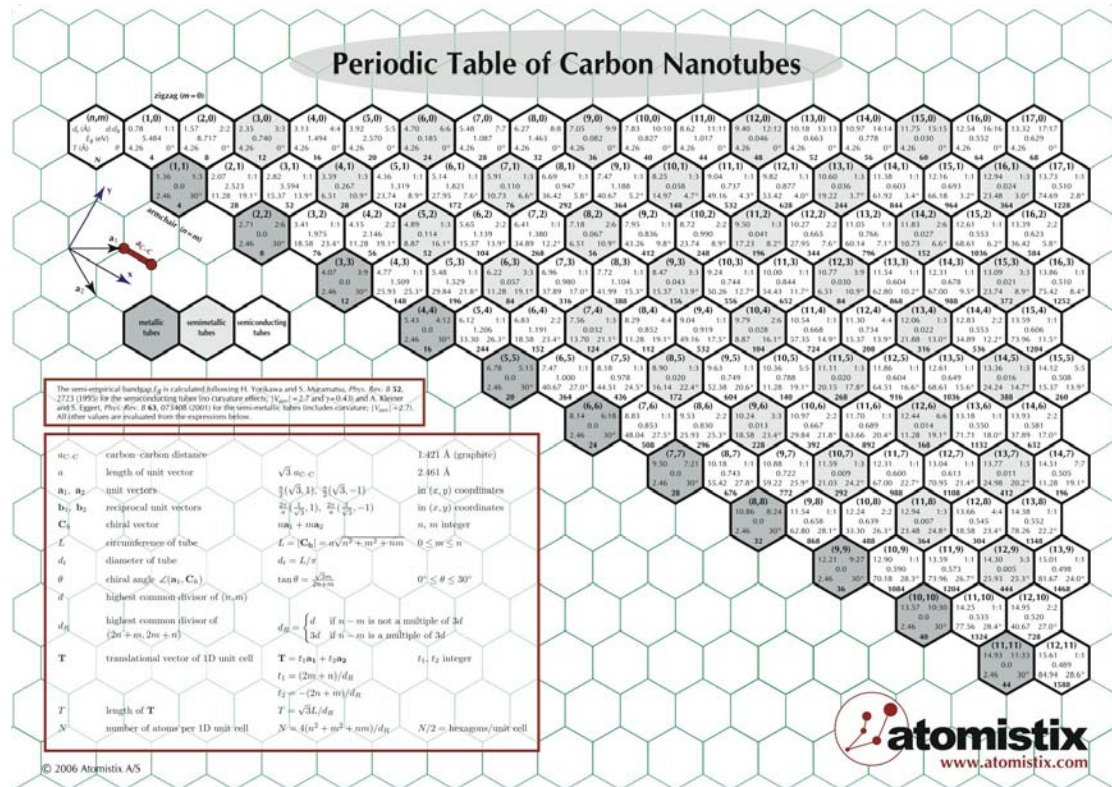
Figure 6. "Periodic Table" of carbon nanotube properties as a function of their *(n,m)* indices. Image © atomistix (www.atomistix.com), reproduced here with permission.
(note to publisher – this needs to be full page landscape in order to read the numbers, a large jpeg version is available)

3. Challenges in electronic carbon nanotube device design

3.1 Standard device designs for carbon nanotubes

Carbon nanotubes are proposed either as building-blocks or as active elements in their own right, in a large variety of nano-devices, ranging from (standard) field-effect-transistors (FETs)[3,4,5,26]- bio-sensors[7,8], opto-electronic devices[27] and nano-electro-mechanical systems (NEMS)[28,29,30]. The first electronic nano-device using CNTs to be built was the common FET with a back-gate (see Figure 7a). In fact, this principle design is still the starting point for almost all CNT-based nano-devices.

In the common FET device design the CNT lies on top of predefined electrodes which themselves are placed on the surface used as dielectric spacer (typically SiO_2 of a few 100 nm thickness) to the back-gate. In later versions of CNT-FET designs developed, the contact electrodes (source and drain) are defined on top of the CNTs for reasons of contact stability, still using a back-gate (Figure 7b). In order to increase gate efficiency, approaches such as top-gates, where the gate was evaporated on top of the CNT were developed[3,31], or aluminium back-gates, which take advantage of the natural aluminium oxide layer (a few nm thick) as dielectric spacer[6]. Concepts for the use of CNTs in 3D integrated device designs have also been proposed where the NTs act as vertical vias between silicon FETs or act as a vertical CNT-FET itself (see Figure 7c,d).

The bridge from a purely electronic CNT-device to a NEMS is then as follows, attempting to keep design as simple to build as possible. The dielectric spacer, as well as the back-gate which lies beneath, can be tailored by selective etching. In this way, several types of NEMSs, such as gigahertz-oscillators[32] or prototypes of non-volatile memories have already been constructed and investigated[33].
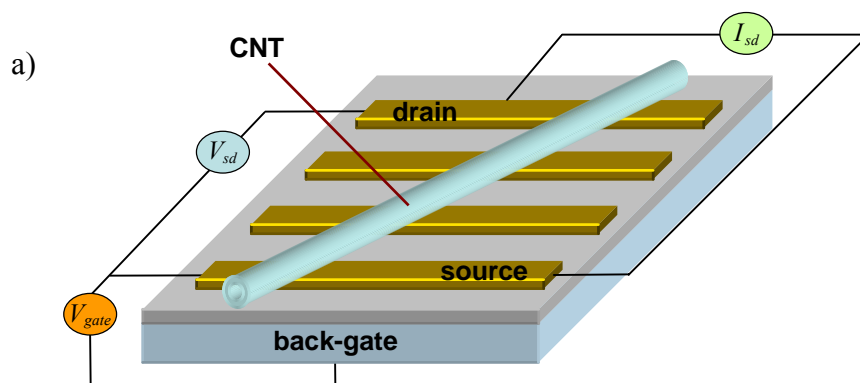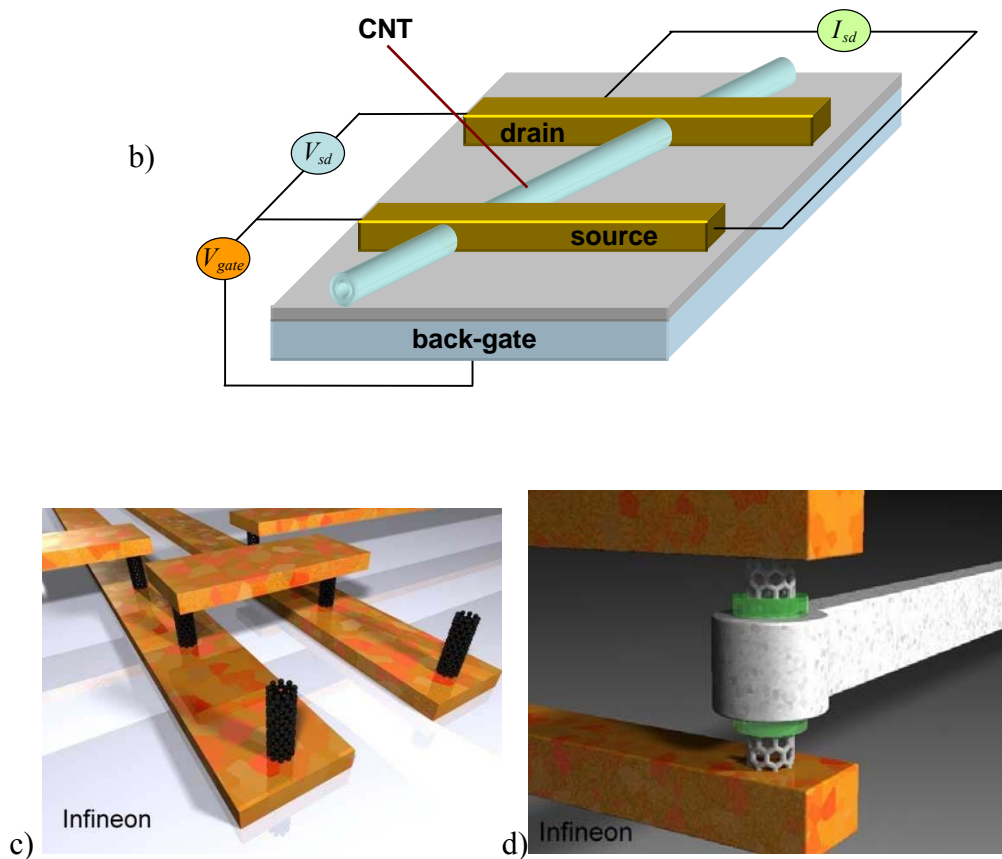
Figure 7. (a) First basic FET design for CNTs with a back-gate. (b) Further development of the FET design shown in (a). The CNT lies now under the contact electrodes, for contact stability reasons. Schematic images showing (c) 'via' complexes and (d) vertical nanotube field effect transistor using CNTs, from Infineon Technologies, reproduced with permission.

3.2 Environmental influence on nanotube electronics

Carbon nanotubes have been shown to be sensitive to the environment. For example oxygen absorption from the surroundings drives CNT devices into a *p*-type conducting state[34,35]. This effect was exploited by IBM[36] to make one of the first controlled nanotube *p-n* junctions. *p*-type conduction in one tube section was achieved through oxygenation, while *n*-type behaviour in the second tube section was achieved through tube surface adsorption of potassium ions[37]. Although this is unlikely to provide an industrial scale solution to controlled nanotube doping it is nonetheless a very elegant proof of concept. Sensitivity to the surrounding gaseous environment, notably gas absorption at carbon nanotube contacts, is something that needs to be carefully controlled in device design, and indeed is under investigation for exploitation nanotube based gas sensors.

3.3 Nanotube positioning

One difficulty for using nanotubes for nanoelectronics is the controlled nanotube positioning on the device. Current techniques include individual tube positioning using AFM[38,39,40,41]. A possibility is to synthesise the nanotubes directly on the device substrates[42,43,44,45]. This last method requires caution to avoid damaging of the device due to the heating required during nanotube growth, and thus there is great interest in lower temperature microwave plasma enhanced growth techniques. Growth has been successfully demonstrated between patterned catalyst particles both vertically, and laterally, and between silicon pillars[46,47]. Within this context there has been interesting work recently on aligned nanotube growth on stepped semiconductor surfaces[48,49]. The catalyst particles attach themselves to the terrace edges and are then pushed along the step edge during growth, leading to controlled highly aligned nanotube growth.

3.4 Controlling nanotube helicity

SWNTs have an enormous potential for application in field effect transistors (FETs). FET devices with nanotubes as conductive channel so far show promising performance comparable to silicon based MOSFETs[50,51,52]. The mixture of metallic and semiconducting nanotubes in bulk material limits the reproducible production of these transistors. It is thus necessary to exert control over nanotube helicity to avoid a random mixture of metallic and semiconducting tubes.

There are no very satisfactory solutions as yet to producing nanotubes with selected helicities. Contacted semiconducting nanotubes can be isolated from metallic tubes

by burning off the metallic tubes at high potential under oxygen flow. At the same time, the semiconducting nanotubes remain intact by applying an appropriate gate voltage which turned the semiconducting tubes insulating[53]. The disadvantage of this method is that the properties of adjacent semiconducting tubes can be affected by burning metallic tubes. A more elegant solution for the isolation of contacted semiconducting and metallic tubes in FET devices is the electrochemical 'over'-funtionalization of metallic tubes[54]. Phenyl radicals, electrochemically generated from diazonium salts, can covalently attach in high densities to the nanotube sidewall. This results in an increase in resistance by several orders of magnitude[55]. During this process, the semiconducting nanotubes remained untouched because of the applied gate voltage which made them insulating.

Rather than removing inappropriate tubes from devices, another approach is to sort the nanotubes before deposition. This has been attempted using solution based chemical selection[56]. Other groups use structure-discriminating surfactants followed by density separation to separate tubes by diameter and electronic type[57]. Krupke *et al.*[58] successfully separated metallic from semiconducting tubes by means of dielectrophoresis. Recent work at Rice University[59] suggests that dielectrophoresis may be a promising way to separate nanotubes, both by electrical properties and also by length.

However none of these offer a way to grow directly *in-situ* appropriate tube types. Within this context there have been recent exciting developments in the field of nitrogen doped nanotubes where results from Cambridge suggest that low levels of nitrogen doping can, under certain circumstances, lead to uniform chirality MWNTs[60].

3.5 Electrical contacts to carbon nanotubes

The electrical contact between a CNT and 3D electron reservoir (contact electrode) is one of the most crucial issues in CNT-based devices.

Already from a purely semi-classical point of view, the different electrostatics indicate that there will be charge transfer from the reservoir to the CNT and vice versa (the CNT is described by quasi-1D, the contact electrodes by 3D electrostatics).

Quantum-mechanically it is the overlap of the 3D wave-function of the contact electrode with the wave-function of the CNT which has a strong 1D character. Notably, the CNTs wave-functions differ also from each other depending on their helicity.

In addition to these problems, the nano-size of the CNT can be a delicate issue. The diameter of CNTs is comparable to the typical grain size of metals, such that differences in the metal work-function in various crystallographic directions come into play. MWNTs naturally suffer less from this problem than SWNTs due to their larger diameter.

An additional problem occurs for semiconducting CNTs. In this case, a Schottky-type barrier between the CNT and the metal arises. This has severe influence on the performance of nanotube-devices such as field-effect-transistors[61]. The working principle of such Schottky-type barrier transistors is different to conventional transistors with ohmic contacts. For example, if in a conventional transistor an ohmic contact is realised to the valence band, the transistor turns on at negative gate voltages (enhanced channel conduction). In contrast a Schottky-type barrier transistor will exhibit an alignment of the Fermi-energy of the metal with the Fermi-energy of the

CNT which lies in the middle of the CNT's band-gap. Such a transistor is ambipolar, turning on at negative and positive gate-voltages due to the thinning of the Schottky-type barrier[61]. Other important consequences for CNT field effect transistors are non-ideal switching behaviour[62] and non-linear scaling relations of the device performance with size-reduction[63].

Currently there are no reliable methods which allow for full control of the contact problem, and research is still ongoing to find proper solutions.

The deliberate doping of both ends of a CNT – to which the contact electrodes are attached – is proposed as a way to overcome this problem[64]. Through this, locally, new (localised) states would be introduced to the CNT's density of states, which could facilitate the transfer of charges between contact and CNT. For semi-conducting CNTs the Schottky-type barrier to the metal electrode would be reduced or in the best case even an ohmic contact achieved.

3.6 Nanotube Junctions

As well as conventional metal-nanotube contacts, it has been shown that certain doping conditions during growth can encourage side branch formation in carbon nanotubes[65,66, 67] but this is not yet well understood or controlled. There has been extensive theoretical modelling of the transport properties of such Y-[68,69,70,71] and T-junctions[72].

4. Doping techniques for carbon nanotubes

The unique morphology of nanotubes means that there are a wide variety of possible approaches to dope them and thereby change their physical and electronic properties

(see Figure 8 below). Many of these take advantage of the molecular nature of the nanotubes, however it is also possible to dope in the more traditional semiconductor industry sense, i.e. deliberately replacing carbon atoms with impurities such as nitrogen. We cover the transport properties of nitrogen doped nanotubes in detail below (Section 5.3) along with their chemical functionalisation behaviour (Section 4.3). For a more comprehensive review of nitrogen doping in carbon nanotubes we refer the reader to References 223 and 73.

The possibility of attaching functional groups to the nanotube surface also allows the combination of the properties of the nanotubes and the addend, as exemplified in Figure 8f,g and h. Different approaches to chemical functionalisation of nanotubes are discussed and described in detail in the following section. We focus particularly on fluorination of nanotubes, since this is a very well developed field covering all subjects from synthesis, characterisation and support by modelling.
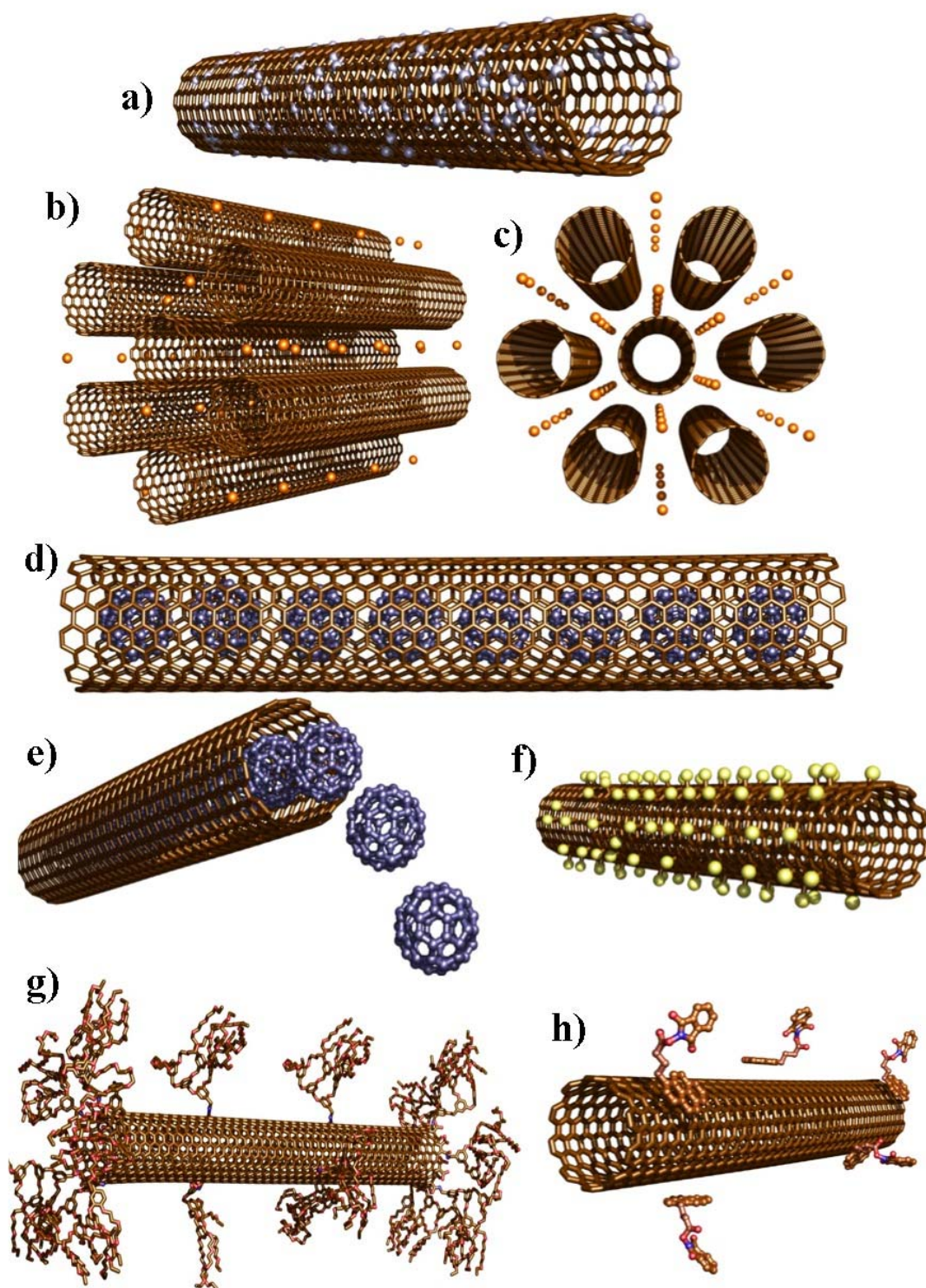
Figure 8. Different approaches to chemical modification of carbon nanotubes. (a) substitutional doped single-walled nanotubes (either during synthesis or by post-growth ion-implantation), (b,c) nanotube bundles intercalated with atoms or ions, (d,e) peapods: SWNTs filled with fullerenes (other endohedral fillings are possible), (f) fluorinated tubes, (g) covalently functionalised tubes and (h) functionalised nanotubes *via* π-stacking of the functionality and the tubes.

4.1 Functionalisation of single-walled carbon nanotubes

Chemical functionalization of single-walled carbon nanotubes (SWNTs) has become an important tool for exploiting their unique physical properties such as electric conductivity, tensile strength and high specific surface. Functionalized nanotubes are promising candidates for reinforced and conductive plastics, sensor and photovoltaic material, scanning probe microscopy tips and much more. Due to the vast number of developed functionalization methods, only some highlights of covalent derivatisation methods for carbon nanotubes and nitrogen-doped carbon nanotubes are discussed here.

In 1998, Chen *et al.*[74] reported the first chemical attachment of organic functional groups to SWCNT materials *via* amide formation between carboxylic acid groups of oxidized nanotubes and amines to obtain nanotube derivatives, which are soluble in organic solvents. The ability to have nanotubes in solution opened the way to manipulate single-walled carbon nanotubes as a bulk material. Since this scientific finding, a vast number of different functionalization methods have been developed, not only to solubilise carbon nanotubes but also to attach functional groups to combine the properties of SWNTs and the addend[75,76,77,78,79,80,81].

The high chemical inertness of carbon nanotubes demands highly reactive species to form covalent bonds with the nanotube sidewalls. This inertness is mainly due to the homogeneous delocalised π-system of the nanotubes. Considering all sp^2 hybridisized carbon allotropes, the chemical reactivity of nanotubes can be placed between the reactivities of fullerenes and graphite (Figure 9A).
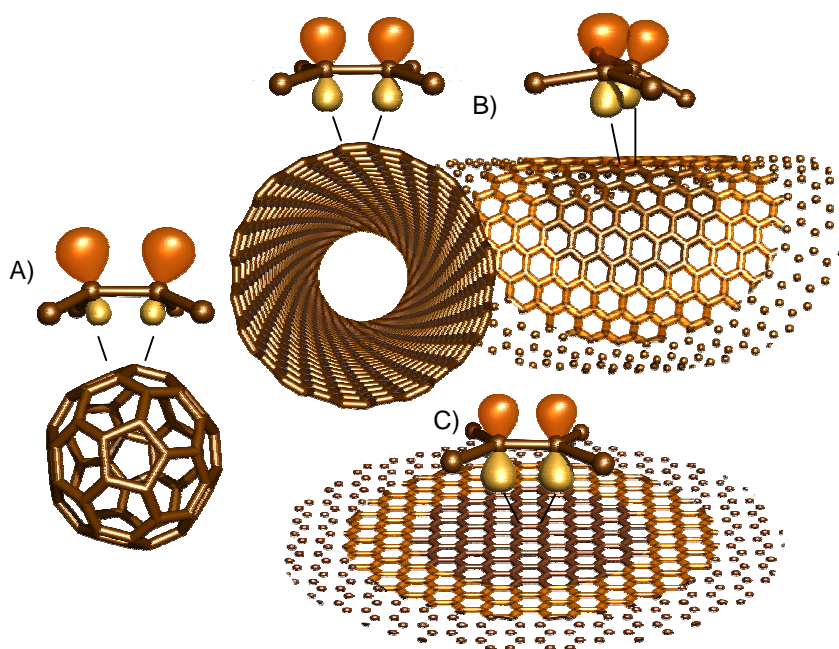
Figure 9. Schematic presentation of the π-orbitals of pyramidalized C=C double bonds A) of a C_{60} molecule, B) a (15,10) SWCNT, and its π-orbital misalignment in comparison with the π-orbitals of a plane C=C double bond of graphene C). The degree of pyramidalization and misalignment indicates the reactivity due to addition reactions.

Graphite is an absolute planar sp^2 hybridized system and all the π-electrons are delocalized (Figure 9C). The change of the hybridisation of the carbon atoms in a graphite sheet from sp^2 to sp^3 increases the strain energy. Fullerenes are curved in two dimensions, whereas a nanotube sidewall is curved in one dimension (disregarding the nanotube end caps). The sp^2-carbon atoms of SWCNTS are bent, as in fullerenes, but only around the tube circumference. The pyramidalization effect of the C=C double bonds parallel and perpendicular to the tube axis is less pronounced than in fullerenes. (Figure 9B). The π -orbitals of the nanotube carbon bonds, angular to the axis, are not only pyramidalized but also misaligned [74,75,82,83,84,85,86,87,88,89,90]. On one hand, the curved π -system of the exohedral region should have an increased electron density compared to planar graphite and therefore a higher reactivity. On the other hand, the driving force of addition reaction, which is due to the loss of strain energy stored in the pyramidalized C-atoms, is much lower than that of fullerenes[75,91].

The logical consequence, that the reactivity of nanotubes decreases with increasing diameter, has been confirmed by theoretical calculations[92].

The remarkable chemical inertness of a perfect SWNT requires highly reactive compounds which can chemically modify the nanotube sidewall. Due to growth conditions, carbon nanotubes can bear so–called defect groups which can be seen as islands with elevated reactivity (Figure 10). Defect groups can be heptagon-pentagon defects, vacancies in the nanotube lattice, or sp^3 hybridized carbon atoms, saturated with hydrogen or oxygen[77]. Oxidation of nanotube material introduces further defect groups such as NO_2-groups, hydroxyls, carbonyls and carboxyls[93,94,95]. The latter is of main interest since these carboxylic acid groups can be further modified *via* the formation of amides or esters. The success of this defect group functionalization method has been the motivation for the development of oxidation processes which form mainly COOH groups out of the sidewall carbon atoms[94,96,97,98,99,100].
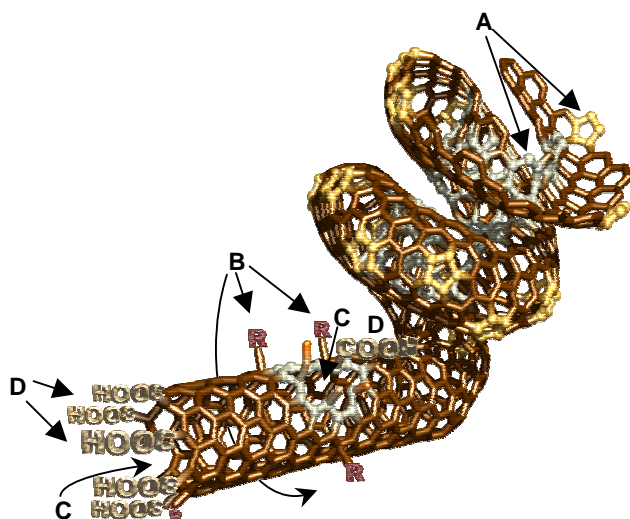
Figure 10. Possible defect groups in SWCNTs: A) Pentagon and heptagon defects (disclinations). These defect groups have not yet been chemically exploited but can lead to nice deformation of the tubes such as tube coiling or Y-shaped tubes (not shown). B) sp^3-defects are formed during the growth process and during oxidation. They are of less interest for functionalization but they are suspected of leading to a partial localisation of the π-system leading to a higher accessibility for addition reactions. C) Vacancies, and their larger cousins holes, lined with functional groups D) Carbon oxides, whereas the carboxylic acid groups are of highest interest for SWCNT functionalization.

Beside the chemical modification of defect groups, other important achievements of sidewall functionalization for single-walled carbon nanotubes are addition reactions using reactive organic species like radicals [101],[102] carbenes[101, 103], nitrenes[101, 104], azomethine ylides[105], lithium alkyls[106,107,108,109], fluorine[110], and diazonium salts[111],[112] (Figure 11A-D, F). In terms of nitrogen-doped single walled carbon nanotubes, less drastic reaction conditions can be used for their sidewall functionalization[113] (Figure 11G).
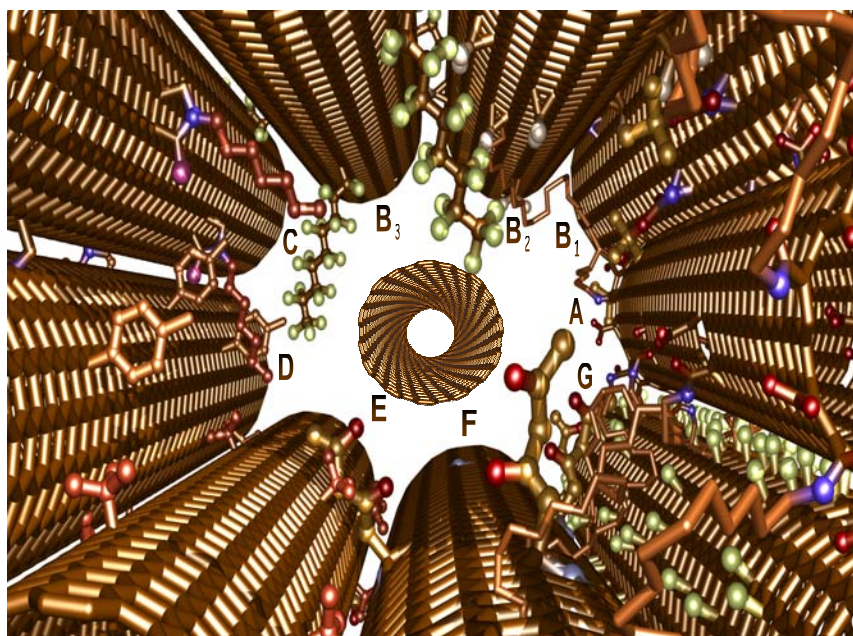
Figure 11. Different methods for the covalent attachment of functionalities to the SWCNT sidewall carbon atoms. A) Formation of amides or esters with the carboxylic acid groups of oxidized SWCNTs. B) addition of nitrenes (B1), carbenes (B2) and radicals (B3). C) [2+3] cyclo addition of azomethin ylides. D) Electrochemical functionalization with diazonium salts E) nucleophilic attack of Lithium alkyls. F) Mannich-type reaction with N-doped single-walled carbon nanotubes. G) Fluorination.

However, control over regio- and chemoselectivity is hard to achieve. For homogeneous functionalization of tubes, the exfoliation and dissolution of the bundles either before or during the attachment of the addends is important. Individual nanotubes in dispersion can be obtained using surfactants[114] and be functionalized later with diazonium salts[115]. Another example for homogeneous functionalized

nanotubes has been reported by Billups and co-workers[116],[117]. There, the nanotubes could be separated due to the electrostatic repulsion after charging with electrons under Birch reduction conditions. Evenly functionalised nanotube samples could then be obtained *via* electrophilic addition reactions with alkyl halides.

4.1.1 Amide / ester formation with carboxylic acid groups of oxidized SWNTs

Amide formation with oxidized single-walled carbon nanotubes is the first reported covalent attachment of an organic molecule to the nanotube sidewall[74].

Oxidized SWCNTs were functionalized with alkylamines, making use of the fact that the SWCNTs possess a high concentration of carboxylic acid groups after oxidation[96,118,119]. The carboxylic acid groups were first converted into acyl chloride groups by treatment with thionyl chloride. The acid chloride-functionalized SWCNTs are then susceptible to reaction with amines to give amides (Figure 12A). The corresponding functionalized tubes show a much higher solubility in organic solvents than the starting material, so their spectroscopic characterization in the liquid phase was possible. In the course of the functionalization, the bundles are split-up into smaller bundles or individual tubes.

More recent publications have shown that the intermediate step of acid chloride formation can be avoided by the reaction with amines at high temperatures (120°C - 130°C) to make non-covalently linked zwitterionic species in high yield[119],[120] (Figure 12C).
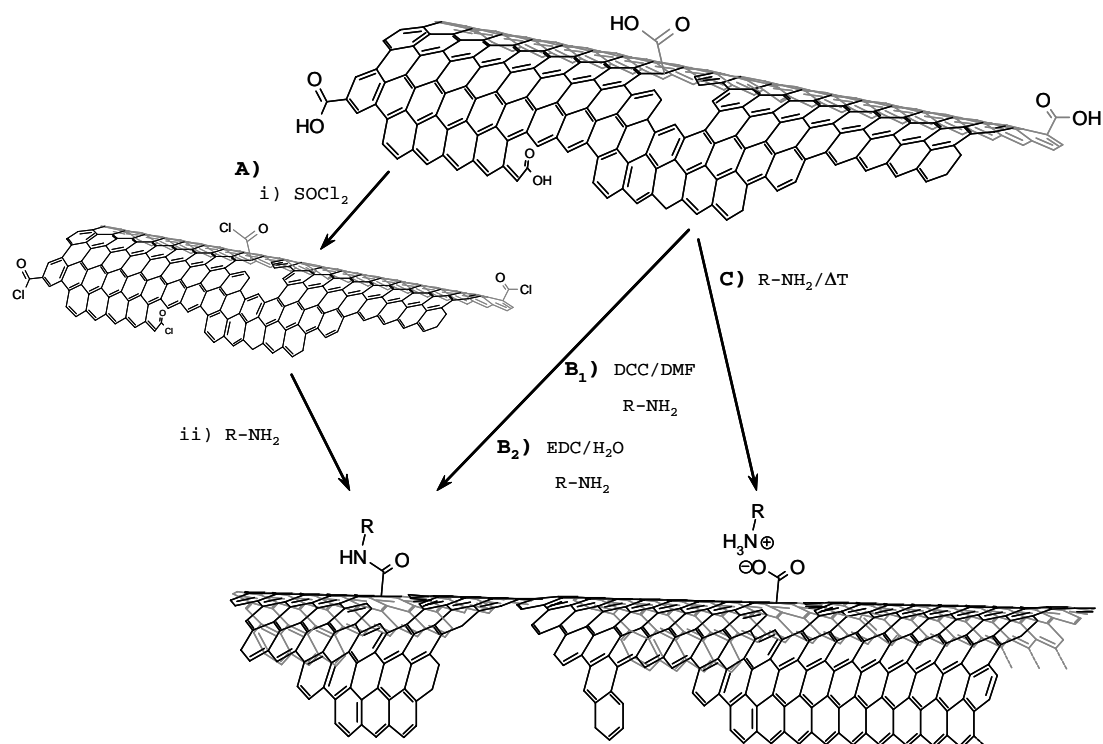
Figure 12. Reaction scheme of the formation of amides with the carboxylic acid groups of oxidized carbon nanotubes and amines *via* A) activation of the carboxylic acid groups by forming acid chlorides with SOCl₂ in an additional reaction step. B) Activation of the carboxylic acid groups using carbodiimides as coupling reagents and C) formation of ammonium carboxylates with amines at elevated temperature.

An elegant alternative of amide or ester formation with the carboxylic acid groups of oxidized SWCNTs is the 'Steglich' reaction. Amides are formed out of carboxylic acid groups and amines *via* diimid derivatives as a coupling reagent. The diimid activates the carboxylic acid group by the formation of an O-acyl urea intermediate which has reactivity comparable to anhydrides. The nucleophilic attack of the amine leads to the amide and urea derivative as by-product, which can be removed by several washing steps after the reaction. One advantage of this amide coupling is that the reaction proceeds under neutral and mild conditions[121]. Another advantage is that oxidized nanotubes can be dispersed with sufficient concentrations in adapted solvents for this type of reaction. For each solvent a soluble carbodiimid derivative is available. For DMF, dicyclohexyl carbodiimid (DCC) is used (Figure 12B) and is now one of the most widely used coupling agent for amidation reactions with

oxidized carbon nanotubes[122]. The ability to also suspend the highly oxidized SWCNTs in deionised water or buffer solutions allowed the formation of SWCNTs with chemically-modified carboxylic acid groups under aqueous conditions[123]. This goal could be achieved with the help of EDC (1-ethyl-3-(3-dimethylamino-propyl)carbodiimide) as a water-soluble coupling agent[124,125].

Following this route, even chemically sensitive biomolecules could be attached to the nanotube sidewall [126]. The large variety of this functionalization method, the availability of reactants, and the feasibility under mild and easily controllable conditions makes amide formation between nanotubes and amines the most common reaction type for obtaining functionalized carbon nanotubes.

4.1.2 Reaction of SWNTs with nitrenes

For the addition of nitrenes, SWNTs were dispersed in appropriate solvents such as 1,1,2,2-tetrachloroethane (TCE) or 1,2 dichlorobenzene (ODCB)[101]. By adding a large excess of an alkyl azidoformate, the nitrenes are generated by thermally-induced N_2 extrusion and react with the nanotube sidewall to give alkoxycarbonylaziridino-SWCNTs. The use of azidocarbonates is necessary for the nitrene addition. Azidoalkyls or –acids tend to undergo intramolecular insertion reactions, forming amines or isocyanates.
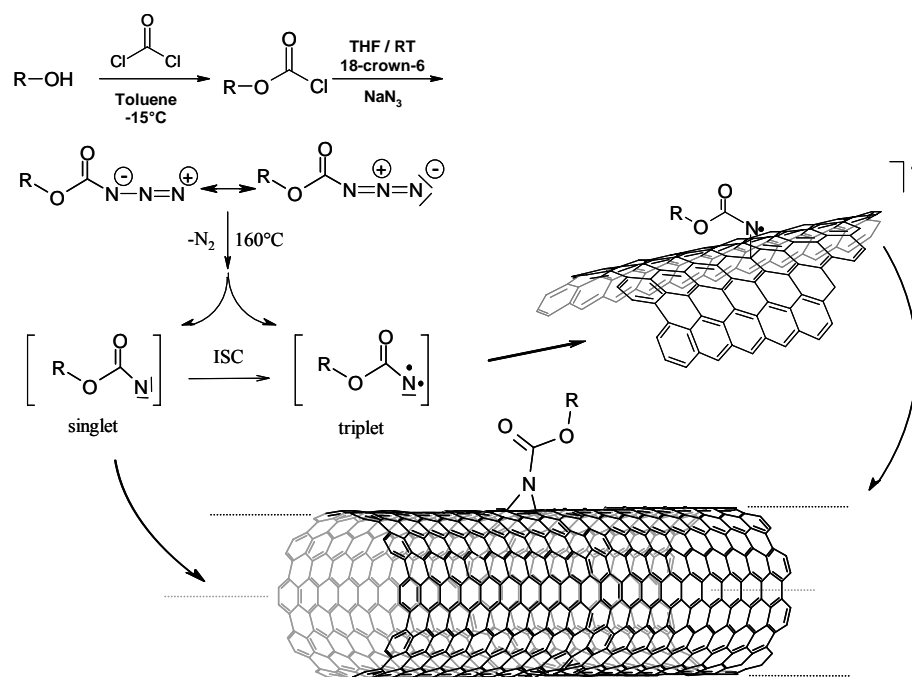
Figure 13. Reaction mechanism of the [2+1] cycloaddition to the SWCNT sidewall.

N_2 extrusion from azidocabonates generates singlet- and triplet-state nitrenes. The singlet nitrenes attack the nanotube sidewall in a [2+1] cycloaddition but can also be transformed into triplet nitrenes by inter-system crossing (ISC). A triplet state nitrene reacts with the π-system of the nanotube sidewall as a bi-radical. Independent to the reaction mechanism, the nitrene addition to nanotube sidewalls results in the formation of an aziridine ring (Figure 13).

With this type of reaction the addition of a large number of organic compounds is possible[104]. The most noteworthy addends which could be attached using this functionalization method are dendrons, which clearly increased the solubility of SWCNTs in organic solvents. Chelating compounds like crown ethers for the complexation of transition metals[104], and alkyl chains, terminated with azido carbonates at each end for the cross-linking of SWCNTs after reaction[127], were successfully attached to the SWCNT sidewall using this reaction type.

Functionalization with nitrenes has potential for the fabrication of nanotube sensors or reinforced materials based on nanotubes. This nitrene reaction has been comprehensively characterized and is a reliable method for nanotube functionalization. However, the harsh reaction conditions and the extreme reactivity of nitrenes only allow the functionalization of SWCNTs with relative inert addends.

4.1.3 Reaction of SWNTs with carbenes

The first addition of carbenes to the nanotube sidewall has been reported by Chen *et al.*[74,96]. The reaction was performed by suspending a SWCNT sample in chloroform-water mixture in the presence of a phase transfer catalyst. Then, the carbenes have been generated with potassium hydroxide.

Another route has been the performance of this reaction with soluble SWCNTs, already functionalized with octadecyl amine (ODA) *via* amide reaction[96]. The modified nanotubes were dispersed in toluene together with phenyl(bromodichloromethyl)mercury ($PhCCl_2HgBr$), the carbene precursor. In both ways, the dichlorocarbenes are formed by α-elimination of chlorine and PhHgBr, respectively. The generated carbene intermediates are strongly electrophil and react with the nanotube sidewall. The resulting SWCNT derivative has been investigated, among others, by XPS where an addition degree of about 1% (2 at% chlorine) has been determined.

The reaction with dipyridyl imidazolidene is a special case for the carbene addition. This compound is the prototype for a "selbstumpolung" capable, nucleophilic carbene[128,129,130]. The carbene is generated by deprotonation of the dipyridyl imidazolium system with potassium *tert*-butanolat[131] (Figure 14).
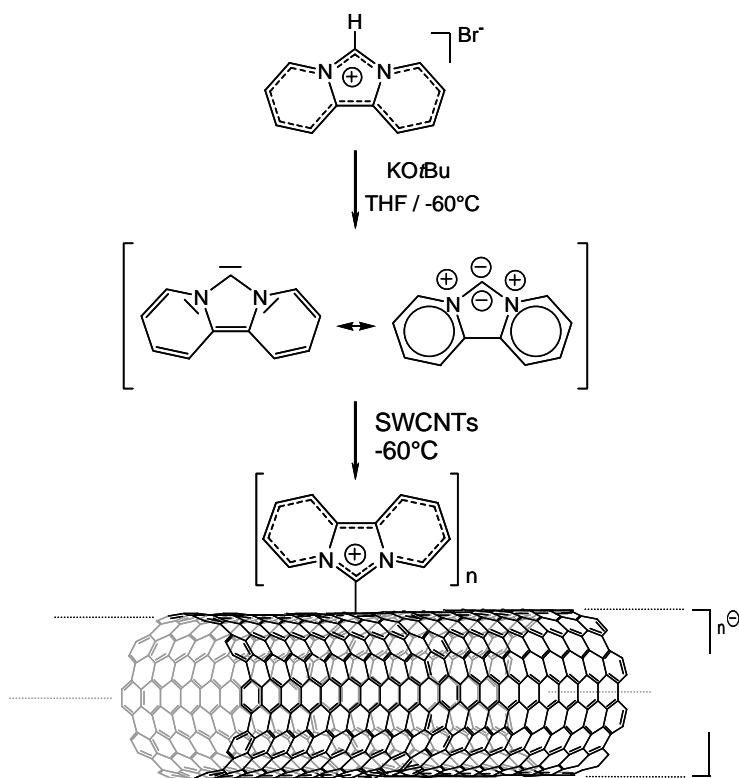
Figure 14. Reaction scheme of the addition of dipyridyl imidazolidene to the nanotube sidewall.

Different to the addition of dichlorocarbenes, this carbene reacts as nucleophil with the nanotube π-system to give zwitterionic 1:1 adducts rather than cyclopropane, which are formed in classical carbene cyloadditions. This univalent attachment is due to the special stability of the resultant aromatic 14π-perimeter of dipyridyl imidazolium cation. The negative charge of this zwitterionic structure has been transferred to the nanotube sidewall resulting in n-type doping of the nanotube sidewall. This offers a further parameter for a controlled modification of the electronic properties of carbon nanotubes (Figure 14).

4.1.4 Reaction of SWNTs with radicals

The first addition of radicals to the nanotube sidewall has been reported by Holzinger *et al*[101]. The radicals have been generated by a photoinduced homolysis of heptadecafluorooctyl iodide, where the formed perfluorinated radicals react with the nanotube sidewall. Like other functionalization methods for single walled carbon nanotubes, the photo induced radical reaction has been transferred from fullerene chemistry[132].

Radicals can also be formed using peroxides like benzoyl peroxide or potassium persulfate as initiator for thermally proceeded reactions. This principle has been used for the *in situ* polymerisation of vinyls like styrene[133], which resulted in a high solubility of the nanotubes in toluene and has a high potential to be used for the fabrication of high performance nanotube composite materials. Benzoyl peroxide itself served also as precursor for phenyl radicals which have been added to the nanotube sidewall[134]. A further evolution of radical reactions with carbon nanotubes to obtain composites with high percolation of nanotubes is an ultrasound induced emulsion polymerization[135].

4.1.5 Reduction of SWNTs with alkali metals

An extensive negative charging of SWCNT sidewalls leads to repulsive interaction where bundles of nanotubes can be split-off into individual SWCNTs. A nanotube sidewall can be negatively charged under 'birch conditions'[136,137]. The reaction process starts with the condensation of ammonia and the dilution of an alkali metal. The uncoloured condensed ammonia becomes dark blue due to the solvated electrons. Under these conditions, the rapid dissolution of SWCNTs indicates a fast reduction of the nanotubes[138]. The highly charged and individual nanotubes can now covalently functionalized by adding alkyl halides[116,117]. An elegant alternative for electron transfer to the nanotube sidewall has been reported by Petit *et al.*[139]. The SWNT

sample was inserted in a quartz optical cell connected to a U-shaped glass tube, where the second branch consists of an ampoule containing organic molecules which serve as electron transmitters. Naphthalene, fluorenone and anthraquinone are such molecules. By adding a piece of lithium, electron transfer from lithium to the organic transmitter molecules results in the radical-anion state of the molecule with Li^+ as the counter ion. This experimental arrangement, developed for *n*-doping of polyacetylene[140], allows the reduction of the SWCNT sample by bringing the solution into contact with the film. The resulting n-doped nanotubes show spontaneous dissolution properties in polar aprotic solvents such as sulfolane, dimethyl sulfoxide (DMSO), *N*-methylformamide (NMF), dimethylformamide (DMF), 1-methyl-2-pyrrolidone (NMP), etc[141].

4.1.6 Reduction of SWNTs with lithium alkyls

The treatment of nanotubes with organolithium compounds leads to the formation of negatively charged single walled carbon nanotubes intermediates R_nSWNT^{n-}. This reaction type for the functionalization of carbon nanotubes has firstly been used for initiating polymerization reactions or to react with functional polymers[106,107,108]. Comprehensive investigations about this n-type doping of SWCNTs have recently been reported by Graupner *et al.*[109]. The SWCNTs were treated with *tert.*-butyllithium (*t*-BuLi) in anhydrous benzene. During the reaction, the inhomogeneous dispersion became a black and homogeneous solution like it can be observed after n-type doping of nanotubes with alkali metals[141]. This observation is consistent with the electron transfer to the SWNTs, accompanied by a nucleophilic attack of *tert.*-butyllithium to the sidewalls of the tubes. The reaction intermediates t-Bu_nSWNTs^{n-} were reoxidized with oxygen to give the un-doped and stable nanotube derivative t-Bu_nSWNT which

precipitated during oxidation. Similar experiments are, again, known from Fullerene chemistry[142]. Compared to fullerenes, the oxidation of negatively charged nanotube sidewall carbon atoms is expected to be even more preferred. The degree of pyramidalization of the C-atoms of SWNTs is lower than that of fullerenes and carbanions prefer a pyramidalized geometry of the central C-atoms. The reformation of the initial strain of pyramidalized sp^2-carbon atoms is therefore less pronounced for nanotubes than for fullerenes[91].
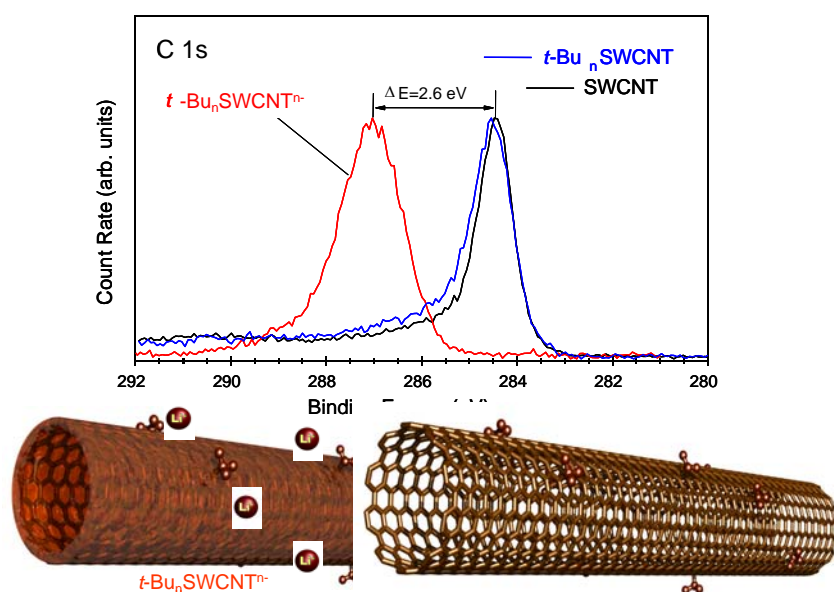
Figure 15. C1s core level of the single-walled carbon nanotube starting material (SWCNT), of the charged intermediate t-Bu$_n$SWCNT^{n-}, and of the reoxidized product t-Bu$_n$SWCNT. Reprinted with permission from Ralf Graupner *et. al.*, J. Am. Chem. Soc. (2006), 128, 6683-6689. © 2006 American Chemical Society.

By repeating this reaction sequence the degree of covalently attached t-Butyl groups increases steadily after every cycle up to a maximum of the carbon-to-addend ratio of 31. This new reaction sequence has been studied in detail by photoelectron spectroscopy. The n-type doping of SWNTs with t-BuLi leads to a clear shift of the binding energy of the C1s core level electrons to higher energies. Subsequent oxidation of the sample leads to a nearly identical carbon 1s core level spectrum of the starting material, indicating the reversibility of this doping process (Figure 15). Using

scanning tunnelling microscopy (STM) at 4,7 K, the *t*-butyl addend could be visualized showing the three-fold symmetry of the addend (**Figure 16**).
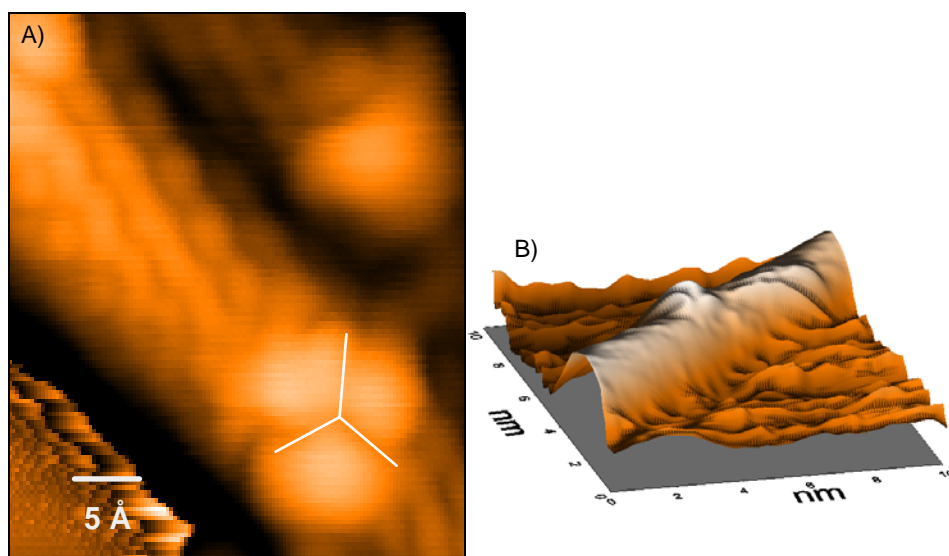
Figure 16. Topographical STM image of *t*-Bu$_n$SWNT with a linear background removed. B) Perspective view of an STM image of an individual *t*-Bu$_n$SWNT. In both images, the three-fold symmetry of the functional group is evident. Reprinted with permission from Ralf Graupner *et. al.*, J. Am. Chem. Soc. (2006), 128, 6683-6689. © 2006 American Chemical Society

4.1.7 1,3- dipolar cycloaddition of azomethine ylides to SWNTs

A further example of a successfully transferred fullerene reaction to the chemical modification of carbon nanotubes has been the 1,3-dipolar cycloaddition of azomethine ylides (Figure 17), generated by the condensation of a glycin derivative and an aldehyde[143,144]. The glycin derivative and the aldehyde form the iminium carboxylate intermediate and after extrusion of carbon dioxide the unstable azomethine ylid is formed and reacts with the carbon nanotube π-system. Pyrrolidino-nanotubes can be synthesized with a wide range of different functionalities by stirring the reaction partner in dimethylformamide (DMF) for several days at 130°C. Using this derivatisation technique, biomolecules could be attached to the nanotube sidewall which served as receptors for biosensors[145]. Light induced electron transfer from attached electron donors to the nanotubes demonstrates

the appropriateness of functionalized carbon nanotubes in photovoltaic cells[146]. A water soluble SWCNT derivative, obtained by this functionalization method, bears a free amino-terminated oligoethylene glycol moiety at the pyrrolidin nitrogen atom. This compound formes supramolecular associates with plasmid DNA through ionic interactions. The complexes were found to be able to penetrate cell membranes[147]. Nanotubes, functionalized by the 1,3-dipolar cycloaddition, could be used and tested as building blocks for nano- and biotechnological applications[148].
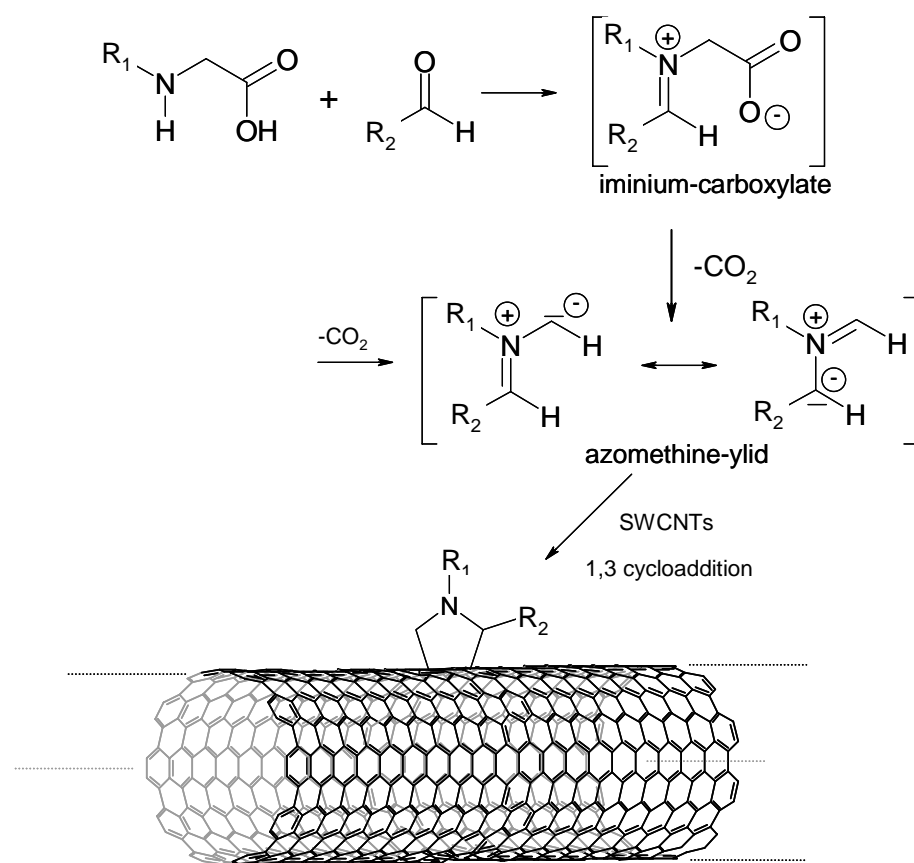
Figure 17. **Reaction scheme of the 1,3-dipolar cycloaddition of azomethin ylides to the nanotube sidewall.**

4.2 Electrochemical modification of carbon nanotubes

A very efficient method for the covalent attachment of organic addends is the grafting of electrochemically reduced aryl diazonium salts, firstly reported by Bahr *et. al.*[111]

38

Contrary to most of the functionalization methods, which have their origin in fullerene chemistry, this type of reaction has formally been applied to highly ordered pyrolitic graphite (HOPG) and glassy carbon (GC) electrodes[149],[150],[151],[152],[153]. A piece of a bucky paper served as working electrode in a three-electrode cell with $Ag/AgNO_3$ as reference electrode and a platinum wire as counter electrode. The electrochemical reaction was carried out in an acetonitrile solution containing the diazonium salt and an electrolyte (tetra-n-butylammonium tetrafluoroborate) at a potential of -1.0 V.

The aryl radical, generated by the reduction of the diazonium salts, reacts with the nanotube sidewall. Then, the nanotube itself becomes a radical like in polymerisation reactions which can further react or be quenched by the solvent. The tendency of the initial aryl radical to polymerize in solution is minimized by the fact that the radical is generated on the surface of the nanotube where the reaction is wanted. This is also the principal advantage of electrochemical functionalization, as opposed to a solution-phase reaction, in which the generated reactive compound can be quenched by the solvent or some other species.
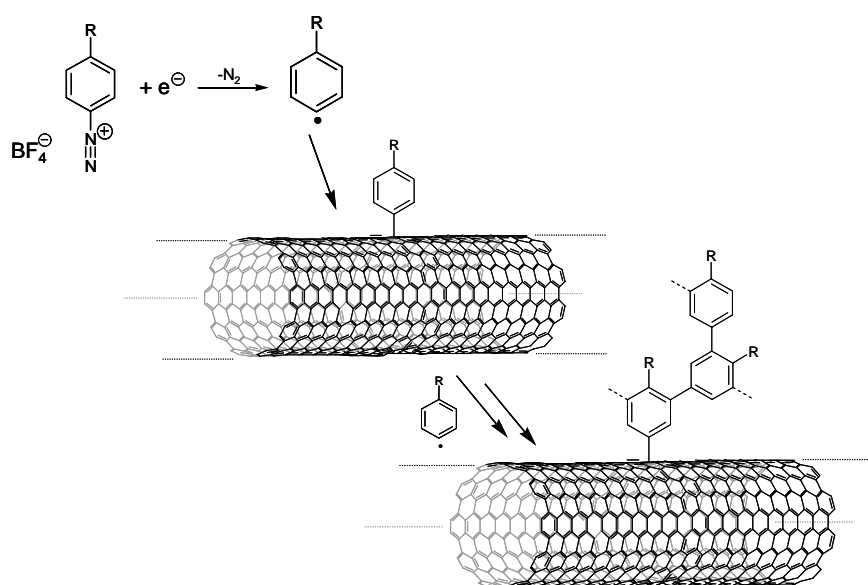
Figure 18. Reaction scheme of the electrochemical functionalization of SWCNTs with diazonium salts and the formations of polyphenylene chains.

For the derivatization of HOPG with the 4-nitrophenyl diazonium salt, McDermott *et al.*[154] proposed polymerization growth where only a few aryl radicals attack the carbon surface, and the following radicals attach to the phenylene addend forming polyphenylen chains (Figure 18).
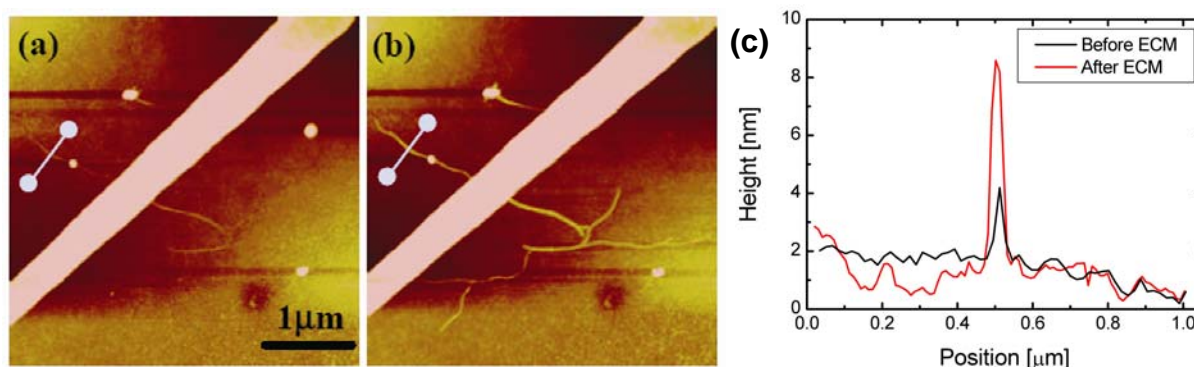
Figure 19. Electrochemical modification (ECM) of an individual electrically contacted SWCNT using a diazonium salt: Atomic force microscope (AFM) images before (a) and after (b) modification; c) line profiles along the lines marked in the AFM images before and after ECM. Reprinted with permission from Marko Burghard *et al.*, Small, 2005, 1, 180–192. © 2005 Wiley-VCH.

The electrochemical polymerization of phenylen radicals on single-walled carbon nanotube sidewalls was investigated by Kooi *et al.*[155]. Individual nanotubes and small bundles were deposited on a glass substrate and contacted with electrodes using electron beam lithography. Reductive functionlaization was performed in DMF at an applied potential of -1.3 V versus Pt with 4-nitrophenyl diazonium tetrafluoro borate as aryl radical precursor and $NBu_4^+BF_4^-$ as electrolyte. After the reaction, only the nanotubes which have been contacted to the working electrode showed an increase of thickness due to the formation of the polymer coating (Figure 19).

Similar results showed the electrochemical experiments under oxidative conditions. 4-aminobenzylamine and 4-aminobenzoic acid have been used as reactants. The oxidative coupling was performed in ethanol with $LiClO_4$ as electrolyte at a potential

of +0.85V versus Pt. The thickness of the polymer coated nanotubes increased linear to the duration of the applied potential. These experiments have been the first approach of an electrochemical manipulation of carbon nanotubes in electronic devices at nanometer scale.

4.3 Functionalisation of N-doped single-walled carbon nanotubes

Since nitrogen-doped single-walled carbon nanotubes are accessible in larger amounts[156], detailed investigation of this material in bulk samples is now possible. The nitrogen in the nanotubes can be seen as regular defects which change the chemical behaviour of the tubes. The reactivity of these N-doped nanotubes can be estimated to be more reactive than un-doped carbon nanotubes of same diameters. Theoretical calculations predict a localization of the unpaired electrons around the nitrogen-defect in the semiconducting hetero nanotubes[157]. In this case, less harsh reaction conditions are possible for the functionalization of doped SWCNT material than for pure single-walled carbon nanotubes[113]. An efficient method for functionalising nitrogen doped carbon nanotubes is the covalent attachement of C-H acidic compound in a 'Mannich'-like reaction (**Figure 20**) which has been applied for the synthesis of heterofullerene derivatives[158]. Pristine n-doped nanotubes, generated by arc discharge, have been dispersed in tetrachloroethane (TCE) together with p-toluene sulphonic acid and acetylaceton. The dispersion was heated to reflux temperature under air flow. Under these conditions, the carbon atoms, neighboured to the nitrogen atoms in the nanotube lattice, are oxidized by oxygen. Acetylaceton adds to the resulting iminium carbo-cations.
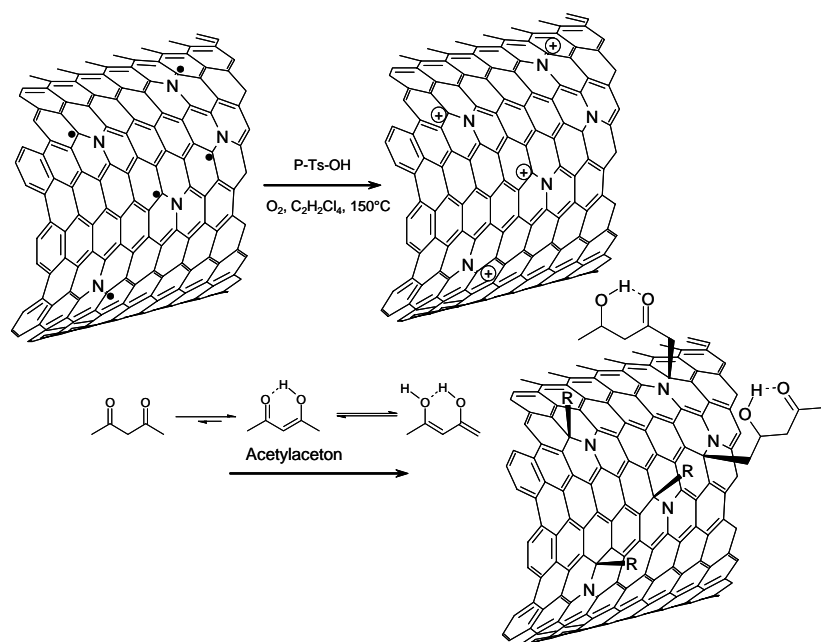
Figure 20. **Reaction scheme of the covalent functionalization of acetylacetone, a C-H acidic compound, to the carbon atoms close-by the nitrogen atoms of the N-doped carbon nanotube sidewall.**

4.4 Fluorination of carbon nanotubes

Fluorination is emerging as an important process for functionalising and chemically activating carbon nanotubes[159,160], with the first fluorination of multi-walled carbon nanotubes performed ten years ago [161], followed by single-walled nanotube fluorination two years later[162]. It takes a special place in the functionalisation methods, as it provides for a high surface concentration of functional groups, up to C_2F without destruction of the nanotube structure. It is an easy and fast exothermic reaction, and the repulsive interactions of the fluorine atoms on the surface debundle the nanotubes, aiding their dispersion. Hydrogen bonds between the fluorine atoms and protons results in high solubility in alcohols or other polar solvents[162, 163], allowing for solution phase chemistry and enabling purification and processing of the nanotubes. Being better electron acceptors than pristine nanotubes, resulting in a better interaction with nucleophilic reagents[164], fluorinated nanotubes can be used as precursors for further functionalisation by nucleophilic substitution[163,165,166,167,168,169]. Subsequent defluorination can be achieved using sonication with anhydrous hydrazine as a reagent[162,163].

There has been much debate on the transport properties of functionalised carbon nanotubes. Despite measurements of decreased conductivity for fluorinated nanotubes[170], the band gap has been predicted to vanish for metallic nanotubes with

an axial fluorine addition pattern[160,171]. The study of the possible addition patterns remains therefore an important issue, and will briefly be discussed below.

Potential applications for fluorinated nanotubes include use in Lithium-ion batteries[172,173,174,175], supercapacitors[176,177] and as lubricants[178,179,180]. Recently, the use of fluorinated nanotubes has been investigated as a new route for polymer reinforcement, where they provide important improvement of the mechanical properties of polymers as compared to pristine nanotube fillers[181,182].

4.4.1 Fluorination Techniques

There are various fluorination methods for carbon nanotubes, including the use of elemental fluorine[161], F_2 gas[183], and CF_4 microwave[184] and RF[168,185] plasma, leading to fluorine coverage of up to C_2F, although under harsh conditions the nanotube material is destroyed[183]. A lower maximum fluorine coverage is observed using BrF_3 vapour[186,187,188] or XeF_2[169,189]. Fluorination is one of the few functionalisation methods that do not necessarily require solvent.

In the case of F_2 gas phase fluorination, the coverage increases with increasing temperature. For single walled nanotubes (SWNTs) the maximum coverage of C_2F is achieved between 250°C and 300°C[190,191]. When the temperature is further increased, nanotubes break down into graphitic material with overall fluorination rate approaching CF[192]. Temperature variant X-ray photoelectron spectra (XPS) show a F1s peak centred at 688eV for temperatures up to 200°C corresponding to semi-ionic bonding, whereas at 250°C there is a shift to covalent bond type with an XPS peak centred at 691eV[190,191]. Both bond types are also observed for energy loss near edge structure (ELNES) in electron energy loss spectroscopy (EELS) studies[177,178,179]. This is reflected in an increase of the F/C ratio from approximately 0.25 at 200°C to 0.5 at 250°C, with an increase of the sample resistivity by a factor three. FTIR spectra shows peaks at 1100 cm^{-1} and 1210-1250 cm^{-1}, correlating with the XPS F1s signals for semi-ionic and covalent C-F, respectively[190,191]. Density functional calculations of the fluorine migration barriers on large nanotube sections showed that this 200-250°C temperature transition corresponds to the barrier for fluorine pairs to migrate to next neighbour sites on the nanotube surface[193].

Plasma functionalisation is the fastest way of functionalising carbon nanotubes; Radio-frequency (RF) plasma with CF_4 gas functionalises carbon nanotubes within seconds to minutes, and depending on the plasma conditions it is possible to either have polymerisation of the monomer on the nanotube surface or covalent functionalisation with coverages up to C_2F[185].

4.4.2 Fluorine Addition Patterns

Theoretical studies to date have concentrated on the maximum C_2F fluorination[164,166,194,195]. Theory predicts axial fluorine addition pattern (see Figure 21a) [160,164,171], apparently in direct contradiction with experimental STM observation of circumferential banding at high coverage[76,166] (see Figure 21b). This discrepancy was explained via "contiguous fluorine addition", where the fluorine axial addition pattern was predicted to form sharp circumferential edges with unfluorinated nanotube sections[196]. In this way, the more stable axial addition still gives rise to circumferential fluorine banding.
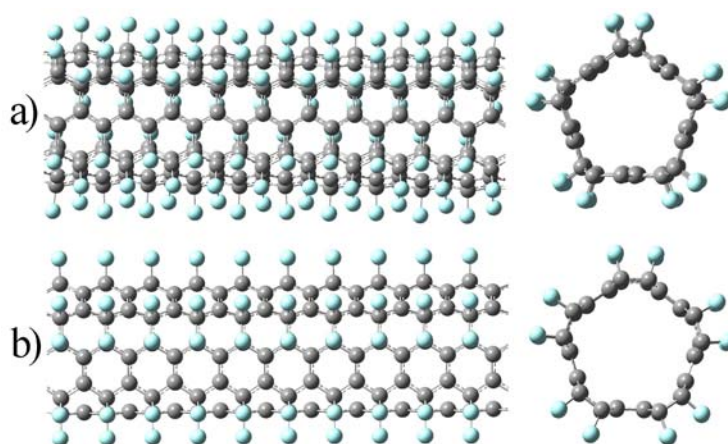
Figure 21: Axial (a) versus circumferential (b) fluorine addition pattern for a (5,5) carbon nanotube.

4.4.3 Conductance of Fluorinated Carbon Nanotubes

Theory predicts that fluorinated armchair nanotubes remain metallic [160,164,171], indeed it has been suggested that fluorination should separate out conduction channels on the nanotube surface, in principle increasing their conductivity[171]. However two-probe resistance measurements of fluorinated SWNT "buckypaper" showed an increase in resistance of six orders of magnitude. It has been suggested that this is due to reduced electrical contact between nanotubes rather than changes of resistance of individual

tubes[162]. Recently, four-probe resistance measurements have shown a decrease of nanotube conductivity by up to two orders of magnitude at room temperature after fluorination by XeF_2 giving 0.8 at% fluorine content, although the fluorinated nanotubes still show metallic character in the temperature dependence of the conductivity[170]. This was however not the case for fluorinated C_{60} peapods, believed to have potential as superconducting material, which behaved as semi-conductors[170]. Zhao *et al.* [197] have shown a decrease in resistivity with increasing heat annealing temperature, due to partial defluorination of the nanotubes. Transport studies of individual fluorinated tubes will be required to ultimately resolve the question of fluorinated tube conductivity.

Fluorinated nanotubes as polymer fillers can also alter the electrical properties of the matrix, for example in SWNT/PAN nanocomposites; composites with pristine SWNTs were highly conducting, while composites with fluorinated SWNTs were not[182].

4.4.4 Fluorinated nanotube chemistry

Their high nucleophilicity can be used to further functionalise fluorinated carbon nanotubes[164]. Also, due to the eclipsed strain from the fluorine atoms being closer than their van der Waals radius, they can more easily be displaced or removed using wet chemistry methods, and the use of fluorinated carbon nanotubes as precursors for further functionalisation enables to add functional groups otherwise unfeasible[181]. Since the electronic properties are drastically altered by the extensive fluorine functionalisation, this opens up new possibilities for using nanotubes as polymer fillers for electronic application. A number of functionalisations have been carried out by fluorine displacement on the fluorinated nanotubes, to produce amino, hydroxyl and carboxyl group-terminated nanotubes. An overview of these methods is presented in reference[181]. Polymer matrices can also be bonded to the nanotubes by partial defluorination, as observed for polyethylene composites[198], opening the door to new hybrid nanotube-polymer composite materials taking advantage of the electronic properties of both host materials.

5. Electronic Transport in carbon nanotubes

5.1 Undoped carbon nanotubes

Electrical transport in undoped carbon nanotubes (CNTs) has been intensively investigated experimentally and theoretically. Conduction in CNTs occurs via the delocalized π-electron system.

At room temperature, both metallic and semiconducting SWNTs are ballistic conductors with two and one spin-degenerate conducting channel(s), respectively[199,200,201]. The channels belong to the first π- and π*-band of the delocalized π-electron system (see also the discussion on the bandstructure of SWNTs given above).

Involving higher bands for transport beyond the first π- and π*-band would require a huge electron excitation energy of the order of 1 eV, equivalent to a temperature of about 1200 K[202]. Thus, at ambient conditions, without external excitation (e.g. incident light), SWNTs only have two spin-degenerate conducting channels available for charge transport. Each of these channels can carry the conductance quanta $G_0 = 2e^2/h$ (e: electron charge, h: Planck quantum)[203]. The energy gap between the conduction and valence bands in semiconducting SWNTs scales inversely with the nanotube diameter (typically around 0.5 eV for a 1 nm diameter tube)[203].

The ballistic conduction of charge carriers in SWNTs is mainly due to the absence of efficient electron-phonon interactions and weak scattering cross-sections for defects in the hexagonal lattice (e.g. pentagon-heptagon dislocation defects). Indeed femtosecond time-resolved photoemission measurements have shown that the mean free path of metallic SWNTs is of the order of several μm[204]. This extraordinarily long mean free path is well above the typical lengths of SWNT based electronic devices, which typically have conducting channel lengths in the sub-micron regime. Thus, SWNTs can be regarded as excellent candidates for low-power consumption molecular electronic building blocks.

With decreasing temperature electron-electron interactions become more important within SWNTs. This is a consequence of their high electronic 1D character, which leads to an effective increase of the Coulomb interaction between the electrons in the nanotube. The electron-electron interactions shift the electronic state of the SWNTs

from a ballistically conducting Fermi-liquid to a correlated 1D electronic system. This state can be described by the Tomonaga-Luttinger formalism. In contrast to a Fermi-liquid, a Tomanaga-Luttinger liquid is characterised by collective charge and spin-excitations[205],[206]. In this state the conductance at source-drain voltages much smaller than the thermal energy (also called zero-bias conductance) follows a power-law dependence with the temperature.

MWNTs consist of a concentric arrangement of different diameter SWNTs which can be either metallic or semiconducting and are of different helicity. Each of these SWNT-shells is principally a ballistic conductor, and thus the resultant MWNTs could also be expected to be ballistic conductors at room temperature with mean free paths comparable to SWNTs. However, the intershell interaction destroys the ballistic conduction properties of each SWNT shell. This can be understood as an electron wave propagating along a SWNT shell having a certain probability to be scattered into a neighbouring shell[207]. From a more theoretical point of view this interaction may be described by an Anderson-type of disorder (random modulations of the nanotube lattice atom potential, but constant in time) in each of the shells[208]. In particular, additional disorder is introduced into each SWNT shell due to incommensurability effects of the different helicities of neighbouring shells[209].

Experimentally, intershell interaction leads to the observation of fractions of the conductance quanta G_0[210]. As a consequence the mean free path in MWNTs at room temperature is considerably shorter than in SWNTs, exceeding at best not more than one to two μm.

Due to the intershell interaction and the fairly large outer diameter, MWNTs exhibit a much weaker 1D character than SWNTs. In fact magnetotransport experiments indicate strongly that MWNTs should instead be regarded as 2D electronic systems[211]. Notably the cross-sections for electron-defect scattering in MWNTs is suggested to be significantly larger than in SWNTs.

Towards low temperatures, temperature-dependent measurements of the zero-bias conductance in MWNTs have also shown a power-law dependence similar to that of SWNTs[212]. Initially this power-law dependence was interpreted to be a finger-print of

the existence of a Tomonaga-Luttinger-liquid state in MWNTs. However, the experimentally observed existence of non-negligible disorder in MWNTs suggests another scenario, since for the development of a Tomonaga-Luttinger-liquid state a well-established ballistic conductance is a necessary pre-condition. This pre-condition is less and less fulfilled for MWNTs with increasing numbers of SWNT-shells and diameter. In the face of these discrepancies several theoretical models have been developed with different explanations for the disorder in MWNTs[207,209],[213]. However, they all introduce only time- and temperature-independent disorder. Concerning zero-bias conductance, Mishchenko *et al.*[213] developed a theory describing a MWNT as a disordered nano-wire with electron-electron interactions and constant relaxation times. The theory provides expressions for the zero-bias conductance for weak and strong disorder degrees. In the limit of weak disorder the power-law dependence of the zero-bias conductance is reproduced, whereas for strong disorder a more complex exponential expression is found. Indeed, zero-bias conductance measurements versus temperature on boron-doped MWNTs showed satisfactory matching with this theory (see also section 5.2 and 5.3)[214].

5.2 Substitutionally doped carbon nanotubes

5.2.1 Nitrogen and boron doped carbon nanotubes

The substitution of carbon atoms in the honeycomb lattice of a CNT by atoms with a different number of valence atoms will in general introduce additional states in the density of states (DOS) of the CNT. Whether these will be electron-donor states, electron-acceptor states, or neither of these two, depends crucially on the local bonding arrangements of the hetero atoms. In the following, we will focus on the most relevant case for electronics, namely graphite-like substitution of boron and nitrogen atoms into the carbon lattice of a SWNT.

Consider first the substitution of a carbon by a nitrogen atom in a graphite-like way into the CNT lattice of a metallic SWNT. Since nitrogen has five valence electrons and carbon only four, the nitrogen state will be located above the Fermi-energy of the undoped SWNT as depicted schematically in Figure 22a. For a SWNT with a diameter of about one nm the nitrogen states will be found approximately a few

hundred meV below the first van-Hove singularity of the π^*-band[215],[216]. The exact position of the nitrogen states depends on diameter, helicity, and number of nitrogen atoms incorporated.

If the incorporated nitrogen ionizes, that is, liberates its excess electron to the π-electron system of the SWNT host, the Fermi-energy will shift upwards in energy relative to its initial position (see Figure 22a).

In Figure 22b the density of states (DOS) for a semiconducting SWNT with a graphite-like incorporated nitrogen is shown. Similar to the metallic SWNT the nitrogen states are found above the initial position (in the centre of the energy gap) of the Fermi-energy. The nitrogen states lies about 150 to 200 meV below the conduction band of a nanotube with a diameter of one nm, depending on the tube helicity and the number of nitrogen atoms.

As the nitrogen states ionize, the liberated electrons will occupy empty states at the edge of the valence-band of the tube and an n-type semiconducting SWNT will be created. Charge transport occurs solely through the π^*-band channel. The Fermi-energy of the nanotube will shift (relatively) upwards in energy and position itself at the nitrogen states in the DOS (see Figure 22b).

The case of boron-doping by substitution of carbon atoms in a CNT is principally the inverse of the nitrogen-doping case. Figure 22c shows the schematic DOS of a metallic SWNT with carbon substituted by boron atoms (graphite-like way). Having only three valence electrons, the boron states will be located below the Fermi-energy of the (undoped) SWNT. Due to their reduced valence compared to carbon, the boron atoms can act as electron traps for the delocalized π-electrons. If these traps are occupied, that is, the boron states are ionized, the Fermi-energy will shift downwards in energy towards the first van-Hove singularity of the π-band. The shift of the Fermi-energy depends on diameter, helicity and number of boron atoms in complete analogy to the case of nitrogen doping. Also similarly to the nitrogen case, the boron states for a one nm diameter SWNT lie some few hundred meV above the first van-Hove singularity of the π-band.

In semiconducting SWNTs, doping by boron substitution in a graphite-like way creates non-occupied states in the energy gap between the initial position of the Fermi energy and the valence-band edge. In SWNTs about one nm in diameter these states lie ~100 meV above the valence-band. If these empty boron-states are occupied, holes at the edge of the valence-band are created and a *p*-type semiconducting SWNT is created. The Fermi-energy will then be found in the DOS at the boron states.

It should be noted that the above descriptions and considerations hold exclusively for graphite-like substitution of carbon by nitrogen or boron atoms. If the substitution is for example in a pyridine-like way and/or accompanied by a structural defect in the carbon honeycomb lattice, it is a priori not clear if additional states in the π-electron DOS will be created, and if so if these will be acceptors or donors.

Finally we note that ionization of dopant states in CNTs is not a trivial task. For ionization to occur the ionized dopant atom has to be electrostatically screened by the surrounding electron sea to conserve charge neutrality. Since SWNTs have a strong electric 1D character, their screening properties are rather poor[217], which is in particular the case for semiconducting nanotubes. The problem of electrostatic screening is considerably reduced in MWNTs due to their larger diameter and the existence of neighbouring SWNT-shells, that is, because they are rather 2D than 1D electronic systems.
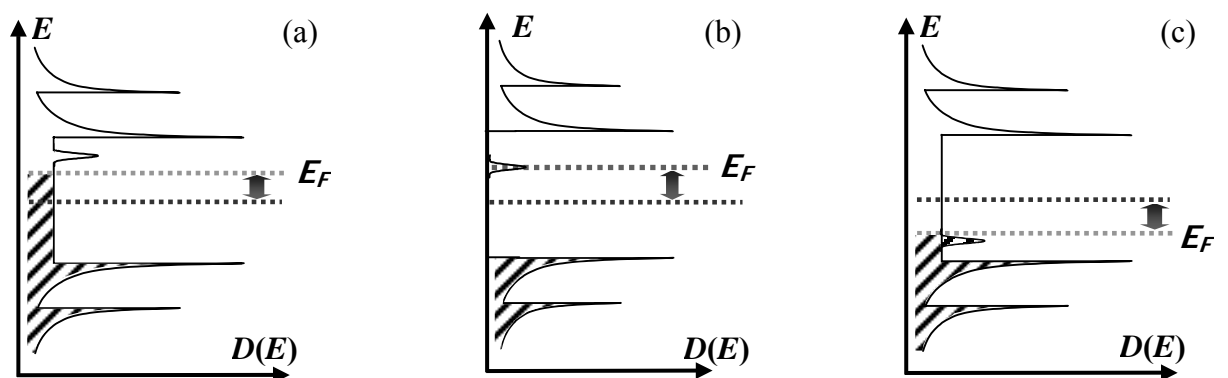

Figure 22. Schematic DOS *D(E)* as a function of energy *E* of a metallic SWNT doped by substitution of carbon by (a) nitrogen and (c) by boron in a graphite-like way. The dotted lines represent the initial (dark grey) and the final (grey) position of the Fermi-energy *E_F* after ionization of the dopant states. The shift is indicated by an arrow. Hatched regions correspond to

5.3 Charge transport theories in carbon nanotubes

5.3.1 Undoped carbon nanotubes

As discussed in Section 5.1, SWNTs are ballistic conductors at ambient conditions. Ballistic conduction can be described within the framework of the Landauer-Büttiker-formalism[218]. In a ballistic conductor the electrons do not suffer from any scattering. The situation is analogous to electromagnetic waves in a wave-guide. In the latter a certain number of transverse modes can propagate the wave-guide depending on the actual shape of the wave-guide. In the case of electrical transport the number of transverse modes, that is, the contributing bands (c.f. previous section); originate mainly from the confinement of the electrons in the conductor. In the case of the CNTs the confinement is given by the translational symmetry around its circumference.

Thus, the total conductance G is proportional to the number of bands available in the ballistic conductor at the Fermi-level times G_0. The conductance quantum $G_0 \approx 19.4$ µS naturally occurs within the Landauer-Büttiker formalism (the reader is referred to the vast literature on this topic). However, the conclusion that the total conductance is given by G_0 times the number of available bands is only valid for perfect transmission of an incident electron wave-function from an electron reservoir (electrical contact/electrode) into the ballistic conductor. In the case that there is a finite probability of the wave-function to be reflected from the conductor/reservoir interface, G is given by the sum over all transmission coefficients T_i. T_i gives the probability that an electron from the reservoir enters in the band i of the conductor. Thus, for a metallic SWNT contacted to two electrodes

$$G = G_0 \cdot (T_1 + T_2)$$

It is noteworthy to stress, that $(G_0 \cdot (T_1 + T_2))^{-1}$ is the contact resistance of the SWNT connected to two reservoirs. It is sometimes misleadingly called the resistance of the

SWNT. If the transmission is perfect then a metallic SWNT has the total conductance $G \approx 9.7$ µS corresponding to a resistance of about 6.4 kΩ.

The confinement in SWNTs is at the origin of the strong 1D character and also responsible for its ballistic conduction properties. This pronounced 1D character of the electronic system has severe consequences at temperatures (well) below room-temperature. In this temperature regime electron-electron interactions come to play and the Fermi-liquid picture, that is, the single quasi-particle picture breaks down. For illustration consider a perfect 1D system of free electrons consisting of a linear chain of length L of equidistant atoms, each of them contributing one electron. In this case the reciprocal space of the linear chain consists also of a linear chain where the Fermi-surface is reduced to two Fermi-points $+k_F$ and $-k_F$. This 1D-topology leads to a considerable difference in the response of the free electron gas to any kind of external perturbation, compared to 2D or 3D electron systems[219].

Consider now an external, time-independent potential $\varphi(x)$ acting on the 1D free electron gas and let $\varphi(q)$ be its Fourier-transform[219]. The perturbing potential leads to a rearrangement of the electron density which may be described by an induced charge density $\rho_{ind}(x)$. The Fourier transform of the induced charge density $\rho_{ind}(q)$ and $\varphi(q)$ are connected through the so-called Lindhard-response function $\chi(q, T)$ with $\rho_{ind}(q) = \chi(q, T) \cdot \varphi(q)$[219]. $\chi(q, T)$ can be determined for wave-vectors q close to $2k_F$ by assuming a linear dispersion relation around the Fermi-energy E_F, $(E(k) - E_F) \sim v_F \cdot (k - k_F)$ [219]. This leads to the expression for the Lindhard-function proportional to $ln|(q+2k_F)/(q-2k_F)|$. Thus, for $q = 2k_F$, $\chi(q, T)$ has a logarithmic divergence which is due to the particular topology of 1D electronic systems. The most significant contribution to the divergence arises from pairs of states, one occupied, the other unoccupied, which are 2 k_F apart from each other[219].

In contrast, in higher dimensions the relative amount of these kinds of states is significantly reduced such that the singularity vanishes. The behaviour of the response-function has important consequences: an external perturbation leads to divergent charge redistributions of the 1D electron system[219] and at $T = 0$ K the electron gas is unstable with respect to the formation of a periodically varying electron charge density (long-range interaction) [219]. In consequence, such an 1D electron system cannot form a stable Fermi liquid as it is known for 3D or 2D metals since the interaction cannot be "hidden" in the effective mass of fermionic single

particles. Further, instead of single particle excitations, only collective excitations are possible[219].

Since the single particle breaks down in 1D electronic systems, the electron system shifts to a correlated state. Depending on the particular properties of the atomic lattice potential either so-called charge- and spin-density wave systems or a Tomonaga-Luttinger-liquid state can develop. A detailed description of all these is beyond the scope of the present overview and the reader is kindly referred to the existing vast and rich literature[205,206].

For the case of SWNTs only the essential and relevant results will be stated here. The zero-bias conductance for SWNTs follows a power-law dependence in temperature,

$$G_{zero\text{-}bias}(T) \sim T^{\gamma},$$

where γ is a measure for the electron-electron interaction strength. In case, the applied voltage V to the SWNT exceeds the thermal energy of the environment of the nanotube the conductance follows the power law

$$G(V) \sim V^{\gamma}.$$

Both power-law dependencies arise from the fact that the density of states of the collective excitations in a Tomonaga-Luttinger liquid follows a power-law dependence, $n(E) \sim E^{\gamma}$, where E is the energy of the excitation[202].

Indeed, Bockrath *et al.*[220] have experimentally demonstrated the existence of a Tomonaga-Luttinger-liquid state in SWNTs by measuring the conductance of individual metallic SWNts in a two-point configuration.

The question on the existence of Tomonaga-Luttinger-liquids in MWNTs will be addressed in section 5.2.3.

5.3.2 Disorder in carbon nanotubes

In the previous section the ballistic nature of the charge transport in SWNTs was discussed. Since ballistic conduction implies the absence of disorder, theories on disordered CNTs mainly address MWNTs[207,209,214]. However, the unit cell of CNTs can be fairly large, that is contain a large number of atoms[203] and thus the theoretical calculations are mainly restricted to "high symmetry" armchair and zig-zag and small diameter (only a few nm or even less) CNTs due to lack of computational power. For

example a (10,10) nanotube has a 40-atom unit cell and a (12,0) unit cell contains 48 atoms, whereas a (10,7) has 143 atoms in the unit cell.

For the same computational power reasons, apart from a very few exceptions (e.g. Ref. 207), most theories assume that charges in MWNTs are exclusively propagated by the outer SWNT-shell. This assumption can be forgotten when comparison to experimental results are made, and misleading conclusions may be derived. Therefore, special care has to be taken in this point.

It is noteworthy that the theories, though nominally developed for MWNTs, are also applicable to SWNTs, because of the assumption that only the outer shell carries a current, and other shells are only there to introduce disorder.

In the following two central carbon nanotube specific theoretical approaches will be sketched and finally the problem of the Tomonaga-Luttinger-liquid state in MWNTs shortly discussed.

MWNTs consist of concentric SWNT-shells. Even under the assumptions that each of these shells are free of defects, the intershell interaction will modulate the atomic potential of each shell, that is, introduce time- and temperature independent disorder. Roche *et al.* developed a theoretical description of the quantum diffusion of electronic wave-packages as function of time on double- and triple-walled carbon nanotubes taking the interaction between two SWNT shells with commensurate and incommensurate pair of indices (or helicities) into account[209]. For example, the zig-zag tubes (7,0) and (14,0) show commensurate helicities, whereas a (10,4) nanotube is incommensurate in helicity with respect to a (6,6) SWNT. However, the theory excludes potential scattering from one shell to another.

The quantum diffusion with time is described within this theory by the time t dependent diffusion constant $D_\psi(t)$. In Figure 23 the calculation results for the commensurate and incommensurate double-walled nanotube (9,0)@(18,0) and (9,0)@(10,10), respectively, and an incommensurate triple-walled nanotube are shown[209].
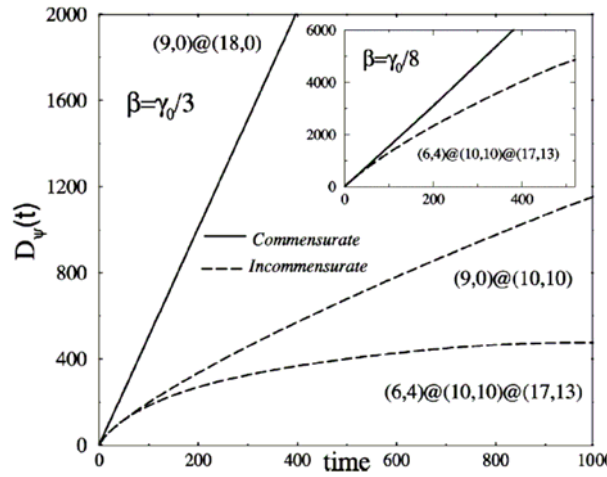
Figure 23. Diffusion coefficients for double-walled and triple-walled commensurate and incommensurate CNTs as a function of time. Time is given in units $h/(2\pi\gamma_0)$, where h is the Planck's constant and γ_0 the tight-binding energy between two neighbouring carbon atoms in the honeycomb lattice. The parameter β is the measure for the imposed interaction strength between neighbouring shells. Inset: Diffusion coefficients for the (6,4)@(10,10)@(17,13) with weaker intershell interaction. Reproduced from [209] S. Roche, F. Triozon, A. Rubio, D. Mayou, *Phys. Lett.* A 285, p. 94 **(2001)** with permission.

The calculation results in Figure 23 reveal that in the commensurate case the wave-package diffuses linearly in time with a constant (average) velocity along the outer shell of the double-walled CNT. That is, the electronic wave-package travels in a ballistic way. In contrast, in the two incommensurate cases $D_\psi(t)$ changes with time indicating a varying average velocity with time. This is the fingerprint of diffusive transport, that is, scattering of the electronic wave-package. In conclusion it can be stated that incommensurable SWNT-shells in MWNTs lead to a diffusive conduction mechanism along the MWNT.

The theory further allows to predict a length L dependence for the total conductance $G(L)$ of the MWNT, $G(L) \sim L^{(\eta-1)/\eta}$, where the parameter η is a measure for whether the conduction is ballistic ($\eta = 1$) or diffusive ($\eta = 0.5$) due to incommensurability effects[209].

It has to be noted that the theory treats conduction in MWNTs in a quasi-particle picture (Fermi-liquid) and does not take electron-electron interactions into account, that is, a possible electronic 1D character of the system.

The consideration of electron-electron interactions versus disorder has been subject of a theoretical work of Mishchenko *et al.*[214]. In this work a MWNT is modelled as a disordered quantum wire with N conducting channels with including electron-electron interaction strength and describing disorder by a constant relaxation time for the electrons. Interestingly, the theory does not make any specific assumptions on the origin of the disorder.

On one hand, the theory can reproduce the main feature of the Tomonaga-Luttinger liquid in the limit of zero temperature. That is, the density of states $n(E)$ of the collective excitations (E: energy) of the correlated electron state in the nanowire follows a power-law dependence, $n(E) \sim E^{\gamma}$ (c.f. also Section 5.3.1) if the Fermi-energy of the system is larger than the effective disorder potential.

On the other hand, in case the effective disorder potential becomes larger than the Fermi-energy of the system, the electron system in the disordered wire with electron-electron interactions can not be any more in a Tomonaga-Luttinger-liquid state. Instead, the density of states $n(E,T)$ of the excitations follows an exponential dependence on energy and temperature. The excitations are still to be regarded as collective excitations (low-energy plasmons), however, with a wavelength smaller than the length of the nanowire. Noteworthy, the theory implies that in a disordered quantum nanowire a crossover from a Tomonaga-Luttinger-liquid state to a disordered state can occur while changing the Fermi-energy and/or the temperature of the system. Also the theory is applicable to metallic SWNTs containing disorder by setting the number of conducting channels to four.

5.3.3 Carbon nanotubes doped by substitutional boron and nitrogen

Boron and nitrogen are the natural choices for doping CNTs since they differ only by one in their number of valence atoms compared to carbon atoms. Thus, a relatively easy incorporation into the carbon honeycomb lattice should be achievable. Indeed, the nitrogen atom, substituted in a graphite-like way was calculated to differ only by 0.01 Å from the equilibrium position of a carbon atom[216]. In contrast boron atoms are considerably smaller than carbon atoms. This produces a higher lattice strain and

consequently a stronger deviation from the atom potential of the carbon honeycomb lattice.

An approach based on tight binding methods correlated to *ab-initio* calculations to describe the electronic transport properties of boron- and nitrogen-doped (graphite-like way) has been performed by Latil *et al.*[221]. This method principally allows for the calculation of relevant transport properties such as the mean free path or conductance scaling for varying concentrations of boron and nitrogen atoms. Pictorially speaking, the approach puts at zero temperature an electronic wave-package on the doped SWNT atomic honeycomb lattice and correlates the time the wave-package needs to diffuse, τ_D, over a chosen length, L_D, along the nanotube with a total length larger or equal to L_D. The main result of this approach is an expression for the conductance (derived from the Kubo formula) which links L_D with the electronic density of states per unit length in the tube, $\rho(E)$, and the diffusion coefficient $D(\tau_D)$,

$$G_0(E, L_D) = 2e^2 \cdot \rho(E) \cdot (D(\tau_D)/L_D),$$

where E is the Fermi-energy position and e the electron charge[221].

In Figure 24, the calculated mean free path as a function of the number of graphite-like boron dopants and diameter of armchair SWNTs is shown. As expected, the mean free path decreases with increasing number of boron atoms and increases with increasing diameter for a fixed number of boron atoms within the SWNT.
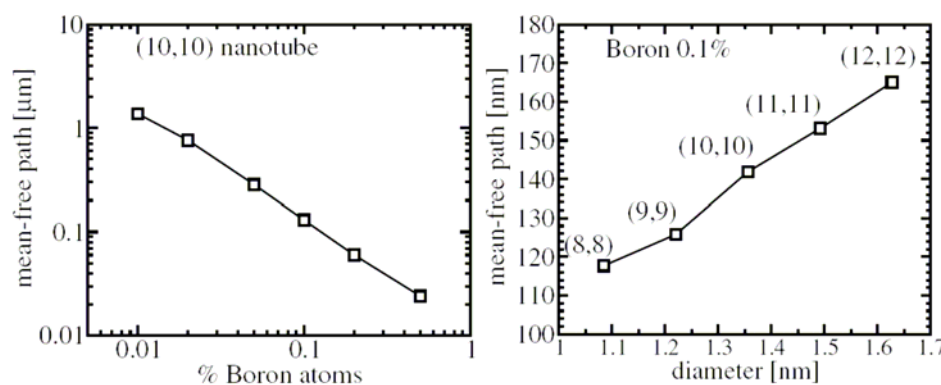

Figure 24.Left: mean-free path of a (10,10) armchair SWNT as function of boron dopants. Right: mean-free path of different diameter armchair SWNTs with 0.1 atom% boron dopants. Reproduced from [221] S. Latil, S. Roche, D. Mayou, J.C. Charlier, *Phys. Rev. Lett.* 92, 256805 (2004) with permission.

The calculated results for the conductance of 0.1 atom% boron and nitrogen doped as a function of Fermi-energy position and different lengths L_D are depicted in Figure 25[221].
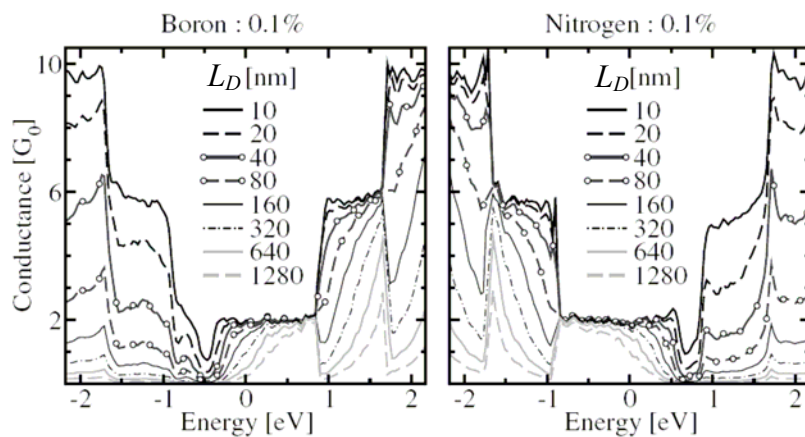
Figure 25. Left: quantum conductance of a (10,10) armchair SWNT with 0.1 atom% boron as function of the (normalised) Fermi-energy position. Right: quantum conductance of a (10,10) armchair SWNT with 0.1 atom% nitrogen as function of the (normalised) Fermi-energy position. Clearly at the energetic position where the nitrogen and boron states are a strong decrease in the conductance occurs due to increased scattering of the current carrying electrons. Reproduced from [221] S. Latil, S. Roche, D. Mayou, J.C. Charlier, *Phys. Rev. Lett.* 92, 256805 (2004) with permission.

It has to be noted at this point that the presented theory does not account for the electronic 1D character of a SWNT. That is, electron correlation has not been taken into account and transport is described in a quasi-particle picture.

5.3.4 Charge transport experiments on boron and nitrogen doped carbon nanotubes

The vast majority of reports on doped CNTs address CNTs doped after synthesis, either by exposure to different gases or in electrolytic liquids (see Section 4.2). This type of post-doping is primarily a gating effect, i.e. the electrostatic environment of the CNTs changes and therefore the CNT Fermi-energy shifts. In particular, this type of doping does not introduce significant disorder to the CNTs, otherwise for example no ballistic conduction at ambient conditions or the fingerprints of the Tomonaga-Luttinger-liquid state could have been experimentally observed in CNTs. The success

or otherwise of electronic doping though chemical functionalization, that is, the addition of side-groups to the carbon lattice, is a topic under debate. There is not yet sufficient experimental charge transport data in the literature on chemically functionalized nanotubes.

Although significant advances have been made in the (recent) past[222],[223],[224],[225] on the *in-situ* synthesis doping of SWNTs and MWNTs through substitution of carbon by boron or nitrogen atoms, there is only very limited electronic transport data in the literature to date.

One of the first transport experiments on substitutionally boron-doped MWNTs (well-graphitised) was reported by Wei *et al.*[226]. In this work individual undoped and boron-doped MWNTs were contacted electrically with two electrodes by focused ion-beam lithography. The resistance of the MWNTs were measured from 300 K to 25 K. In Figure 26 the natural logarithm of the resistivity ρ (calculated on the basis of the resistance measurements and the dimensions of the MWNT sample) versus inverse temperature is shown. Linear behaviour was observed for both undoped and boron-doped tubes, interpreted as thermal activation of electrons from valence to conduction or dopant states and/or as thermally activated interlayer hopping of electrons between SWNT-shells in the MWNT. Later, Cerw *et al.* [227] reported on resistance measurements versus temperature on individual boron-doped MWNTs. The results were also interpreted within the framework of a hopping conduction mechanism.

Despite the similar interpretation of the transport in boron-doped MWNTs, the hopping conduction interpretation fails to explain the experimental data for temperatures above a few ten K, since the hopping theory should cover the whole experimental temperature range. Moreover, hopping conduction would require charge transport by transferring charges from one localised site to another localised site. Referring to the discussions in the previous sections on the electronic properties of doped CNTs such rather strongly localised sites are very unlikely to exist.
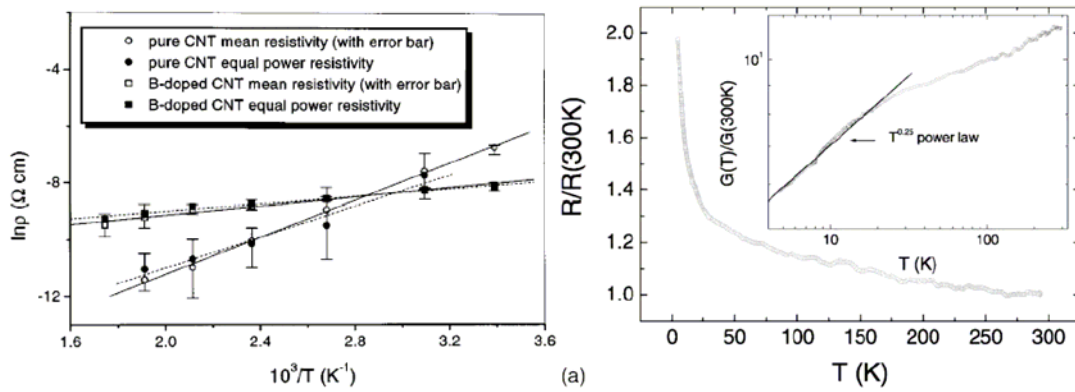
Figure 26. Left: Natural logarithm of the electrical resistivity of undoped and boron-doped nanotubes as a function of inverse temperature, ref. [226]. The equal power resistivity takes Joule heating into account (lines: linear fits to the data). Right: Resistance of an individual boron-doped MWNT as a function of temperature, ref. [227]. The inset fits the conductance to an exponential function vs. temperature and yields an exponent of 0.25. Reproduced from [226] B. Wei, R. Spolenak, P. Kohler-Redlich, M. Ruhle, E. Arzt, *Appl. Phys. Lett.* 74, p. 3149 (1999) and [227] R. Czerw *et al.*, *Curr. Appl. Phys*. 2, p. 473 (2002) with permission.

This apparent inadequacy in the interpretation of the results could be resolved by measurements of the zero-bias conductance of MWNTs doped with approximately 1atom% boron dopants as a function of temperature[214]. In Figure 27 the zero-bias conductance of an individual boron-doped MWNT is show. The dashed line represents a fit following the Tomonaga-Luttinger-liquid theory[202], the continuous line is based on the theory of a disordered wire[213] with N conducting channels in case the Fermi-energy is smaller than the effective disorder potential (c.f. to the discussion in Section 5.3.2). In this case, the temperature dependence of the zero-bias conductance follows an exponential law[213]. Obviously the experimental data are significantly better fitted by the disordered wire theory. In particular, the theory covers the whole experimental temperature range.
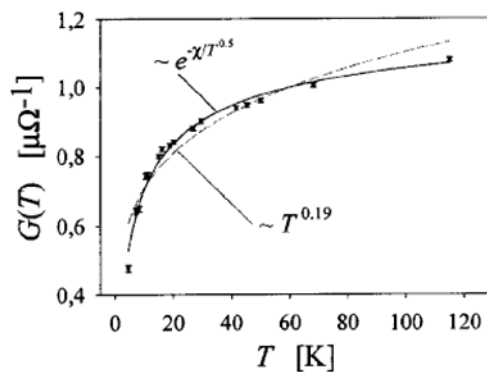

Figure 27. Temperature-dependence of the zero-bias conductance for an individual boron-doped MWNT. The fit assuming a disordered conducting wire with $G(T) \sim \exp(-\chi / T^{0.5})$ accounts for the experimental data considerably better than the fit which assumes a Tomonaga-Luttinger-liquid

state with $G(T) \sim T^{0.19}$. The parameter $\chi = 1.88 \pm 0.07$ K$^{0.5}$ is a measure for the electron-electron interaction vs disorder strength in the boron-doped MWNT. Reproduced from [214] V. Krstić, S. Blumentritt, J. Muster, S. Roth, A. Rubio, *Phys. Rev. B* **67**, 041401(R) (2000) with permission.

A more detailed analysis revealed further that the conductance of the boron-doped MWNTs scales at room temperature with length following the form $G(L) \sim L^{(\eta-1)/\eta}$ (c.f. Section 5.3.1) and that transport is diffusive ($\eta = 0.49 \pm 0.1$)[214]. The origin of the diffusive conduction mechanism can be attributed to an existing incommensurability between the SWNT-shells in the MWNT and the subsitutional boron dopants.

In the previous sections the principal differences between charge transport in MWNTs and SWNTs have been already stressed. One of the primary differences is that SWNTs have no intrinsically occurring source of disorder (no intershell interaction). Also, the experimental observation of ballistic transport in SWNTs[199,200,201] at room temperature indicates that lattice defects have a relatively small scattering potential. Therefore, the question arises of what strength the disorder potential would be due to the substitution of carbon by boron atoms in a SWNT. Again the zero-bias conductance is the best charge transport measure to detect disorder influences of the substitional boron dopants in a SWNT.

In Figure 28 the zero-bias conductance of an individual boron-doped, metallic SWNT is shown as function of temperature in a double-logarithmic plot[228]. The boron content is not more than 0.1 atom% in contrast to the reported 1 atom% in MWNTs. The boron-doped SWNT is contacted by metal electrodes, which have been defined on top of the tube. The Fermi-energy, lies, as expected, within the π-band (*p*-type conduction), that is, the current carrying electrons are relatively close to the boron states in the DOS.

The temperature dependence of the zero-bias conductance does not follow a power-law behaviour (dotted line) as would be expected for a Tomonaga-Luttinger-liquid like state. Instead the experimental data are better fitted by a disordered theory (dashed line), although non-negligible data fluctuations are present. The fluctuations are suggested to originate from the enhanced scattering cross-section for the current carrying charges with the boron dopants, since both are lying energetically relatively close within the DOS. The circumstance that the fluctuations occur while changing temperature suggests further, that the scattering mechanism is (though probably weakly) temperature-dependent.
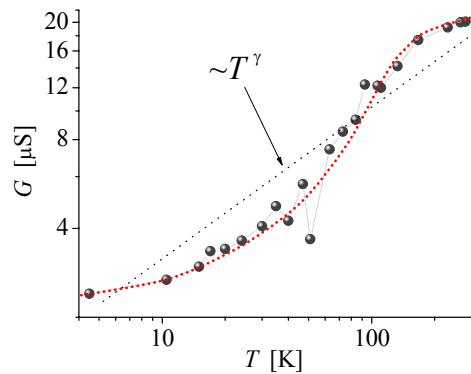
Figure 28. Zero-bias conductance of an individual boron-doped, metallic SWNT is shown as a function of temperature in a double-logarithmic plot. The boron content is less than 0.1 atom%.

For nitrogen-doped MWNTs and SWNTs even less experimental (direct) electrical transport data are reported than for boron-doped CNTs. The vast majority of the literature on transport in nitrogen-doped CNTs is theoretical calculations.

Choi *et al*. [229] reported one of the first electrical transport and thermopower measurements on mats of nitrogen- and boron-doped MWNTs. The morphology of the boron-doped MWNTs was well-graphitised, that is, the MWNT consisted of SWNT shells. In contrast the nitrogen-doped MWNTs showed additional bamboo-like features, but concentric shells of SWNTs were still apparent[229].

The thermopower measurements revealed that the majority charge carriers in nitrogen-doped MWNTs are electrons. That is, an *n*-type-conduction is principally achievable in MWNTs via substitutional doping. In Figure 29 the resistance of the mats as a function of temperature is shown[229].
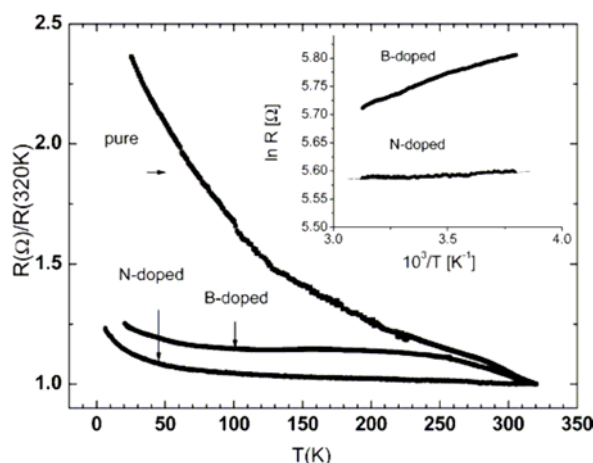
Figure 29. **Temperature dependence of the resistance _R_ for pristine, boron-doped and nitrogen-doped MWNTs mats (two-probe measurements). In all three cases a non-metallic behaviour is observed. Inset: logarithm of _R_ versus reciprocal temperature, indicating that the dominant transport process in the mats is a hopping process. Reprinted with permission from [229] Y. M. Choi et al, Nanoletters 3(6), 839-842 (2003), copyright 2003 American Chemical Society.**

The resistance in the doped MWNT mats increases only slightly relative to the undoped MWNT mat. The plot in the inset indicates that the charge transport through the mats is dominated by a hopping mechanism. The results are understood, taking into account that in mats or networks of nanotubes, the main barrier for the charges is not within the tubes, but is the hopping from one tube to another. It is noteworthy that the doping of MWNTs by substitution with nitrogen and boron reduces the inter-tube hopping barrier.

One of the first reports on the application of nitrogen-doped MWNTs for field-effect transistors was that of Xiao _et al._[229]. They fabricated a field-transistor using an individual nitrogen-doped MWNT and could show that the device acts as an _n_-type transistor. However, their MWNTs were rather large in diameter (around 50 nm) and were not well-graphitised[229]. That is, the MWNTs consisted mainly of a chain- and bamboo-like structure, and almost no concentric SWNT-shells were observed[229]. Thus, although an _n_-type conduction could be achieved, no reliable conclusions on the influence of nitrogen-doping of well-graphitised MWNTs can be drawn.

In the case of boron-doped SWNTs it was demonstrated that even a small concentration of boron dopants can have dramatic influence on the electrical transport properties. One of the reasons is the considerably smaller size of a substitutional boron atom in a carbon honeycomb lattice compared to a carbon atom. The induced

lattice strain enhances the effective scattering cross-section of the boron dopant. In contrast, nitrogen atoms substituted under the same conditions differ only slightly in size from the carbon atoms[215]. Therefore, a smaller lattice strain is apparent, and thus no significant enhancement of the nitrogen scattering cross-section is to be expected. As a consequence electrical transport for charge carriers being energetically well separated from the nitrogen dopant levels in the π^*-band should not suffer from scattering (c.f. also to the discussion in section 5.3.2).

To test this hypothesis the most suitable way is to measure the temperature-dependence of the zero-bias conductance of a nitrogen-doped, metallic SWNT in its *p*-conducting state. That is, the Fermi-energy lies within the π-band. In Figure 30 the zero-bias conductance of a nitrogen-doped SWNT, with 1 atom% dopants, under these conditions is shown[230]. The plot is in double-logarithmic representation. The dotted line corresponds to power-law dependence, fingerprint of a Tomonaga-Luttinger-liquid state. Obviously, the data points deviate from this dotted line. The data are better fitted by the dashed dotted line. This fit is based on a disordered nanowire, similar to the case of the boron-doped MWNTs and SWNTs. This experimental result is surprising since it is not necessarily theoretically predicted (c.f. to the previous sections). A possible solution would be to take into account a more long-ranged interaction between the nitrogen dopant atoms and the current carrying charges. Indeed, electron-energy-loss results showed the existence of differently substituted nitrogen atoms, graphite- and pyridine-like[222,223]. The pyridine-like nitrogen is expected to have a permanent electric dipole moment which acts as additional scattering mechanism for the current carrying electrons[230]. In fact the fit representing the dashed dotted line in Figure 30 takes this electrical dipole interaction into account[230].
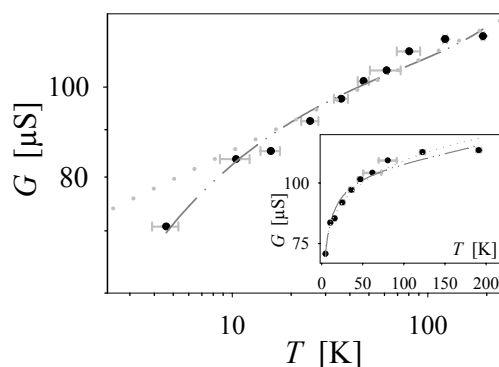

Figure 30. Temperature dependence of the zero-bias conductance of an individual, nitrogen-

doped (metallic) SWNT. The dotted line corresponds to a power-law behaviour. The dash-dotted line to assumes a disordered wire system with electric-dipole interaction. Inset: Same data with linear axis. Reproduced from [230] V. Krstić *et al.*, cond-mat/0601513, with permission.

The experiments on the boron- and nitrogen-doped MWNTs demonstrate that these types of CNTs exhibit relatively strong disorder already at room temperature and as a consequence any notable ballistic conductance at room temperature is suppressed. However, the situation turns out to be different for nitrogen- and boron-doped SWNTs. Electrical transport measurements on individual nitrogen- and boron-doped metallic SWNTs have shown that even at room-temperature ballistic conductance over lengths over several hundred nm is possible even with 1 atom% of dopants[228,230].

The interest in nitrogen and boron-doped CNTs in terms of application is the control of the type of charge carriers within the carbon nanotubes. This control is one key-issues for a successful implementation of CNTs in nano- and molecular-electronics. Another key-issue is the power-consumption of a potential device (e.g. field effect transistor) based on doped CNTs.

For doped MWNTs the control on *n*- and *p*-type conduction seems to be achieved. However, doped MWNTs show a high degree of disorder which has two important consequences. The increased scattering of charge carriers increases the power consumption of the device and at the same time increases Joule heating. The latter is of particular importance because it can lead to device malfunction and in the worst case to failure in a comparably hot environment (e.g., CPU or VIA in integrated circuits).

In contrast, nitrogen- and boron-doped SWNTs still exhibit ballistic conduction at ambient temperature over several hundred nm. Thus, the power-consumption and the risk of malfunction of devices based on doped SWNTs are significantly reduced compared to doped MWNTs. But SWNTs are more sensitive to influences from the environment (gases) due to their 1D character and suffer from a higher work-function mismatch with typical electrical contact materials like gold or copper. In particular the latter may impede the creation of *n*-type-conduction due to electron extraction from the nanotube.

6. Conclusions

It is clear that the full story of electronic transport in individual single and multi-walled carbon nanotubes, and in particular their doped counterparts, is still a long way from completion. The wide range of possible nanotube pre- and post-growth treatments, and difficulty of conducting transport studies at this scale, mean that further work is needed. Nonetheless there is already sufficient studies to show the potential promise of these remarkable materials.

When considering doping of carbon nanotubes it is important to remember that nanotubes are not currently a homogenous material. Depending on whether they are single- or multi-walled, their properties change radically. Within this, single-walled nanotubes can be metallic or semi-conducting depending on their helicities. Samples normally contain a statistical distribution of tube lengths, diameters, and number of tube walls. In addition nanotube samples are of varying purity, normally including other materials such metal catalyst nanoparticles, amorphous carbon (both distributed throughout the sample and coating the nanotube walls), absorbed surface oxygen, and surface silicides, depending on the growth technique employed. As well as affecting the fundamental properties of the nanotubes themselves (for example absorbed oxygen plays a role in p-type behaviour of 'pristine' nanotubes[231]), these impurities can also affect gate properties when using nanotubes in transport devices and can modify, e.g. absorption properties of gas species (important for interpretation of gas sensor studies). Thus care must be taken to separate out measurements on individual nanotubes from secondary surface effects due to impurities.

Equally this means that one must pay careful attention to the applicability of bulk characterization techniques to nanotube samples. Fourier Transform infra-red spectra (FTIR) and Raman spectra will also include strong signals from amorphous carbon, and surface sensitive techniques such as XPS are especially sensitive to extraneous information from isolated amorphous carbon as well as surface coatings on the nanotubes. For this reason nanoscale probes allowing study of individual nanoobjects, such as spatially resolved electron energy loss spectroscopy (EELS) using scanning transmission electron microscopy (STEM), are particularly important for characterization of doped nanotube samples. However in this case results must once

again be treated with care due to the sensitivity of the nanotubes to the electron beam, which can quickly lead to amorphisation of the sample, local build up of additional amorphous carbon material, and structural change in highly nitrogen doped regions of the tubes[232].

Doping of carbon nanotubes presents a number of opportunities and complications compared to bulk doping of conventional semi-conducting materials. As 1D molecular wires, they have a range of possible surface doping techniques such as gas absorption (physisorption, chemisorption and π-stacking), binding of complexes to intrinsic defects such as vacancies, metal coating, etc. However in heteroatom doped CNTs the doping sites are often the most chemically active in a system, and since single walled nanotube sites are all surface accessible this means that properties of doped nanotubes can change over time as heteroatoms react with their environment.

It is clear that the role of carbon nanotubes in nanoelectronics is likely to change radically as our technological control over growth, manipulation and functionalisation of the tubes improves. At the same time we are developing understanding and control of gating and contact processes. Research is advancing rapidly in many parallel fields, and it should hopefully soon be possible to achieve controlled growth or arrangement of nanotubes of specified diameter, length and helicity onto chip surfaces. This will open the door to micro processors with smaller component sizes, faster switching speeds, improved thermal management and decreased leakage. Molecular nanotube-based computing offers the potential for novel device design including mecano-electronic data storage, and ultimately opto-electronic nanotube based devices.

Carbon nanotube doping can be achieved using a variety of non-conventional techniques that exploit the molecular, high surface area nature of the material. As these develop beyond the laboratory and into industrial applications, it seems clear that there is a bright future for carbon nanotube based nanoelectronics.

Acknowledgements

[1] R. S. Ruoff, D. C. Lorents, *Carbon* 33 925-930 **(1995)**

[2] P. Kim, L. Shi, A. Majumdar, P. L. McEuen, *Phys. Rev. Lett.* 87 215502 **(2001)**

[3] A. Javey, H. Kim, M. Brink, Q. Wang, A. Ural, J. Guo, P. Mcintyre, P. McEuen, M. Lundstrom, H. Dai, *Nat. Mater.* 1 241 **(2002)**

[4] A. Javey, J. Guo, Q. Wang, M. Lundstrom, H. Dai, *Nature* 424 654 **(2003)**

[5] S.J. Tans, A.R.M. Verschueren, C. Dekker, *Nature* 393 49 **1998**

[6] M. Radosavljevic, M. Freitag, K.V. Thadani, A.T. Johnson, *Nano Lett.* 2, p. 761 **(2002)**

[7] J. Kong, N. Franklin, C. Zhou, M. Chapline, S. Peng, K. Cho, H. Dai, Science 287, 622 **(2000).**

[8] J. A. Robinson, E. S. Snow, S. C. Badescu, T. L. Reinecke, F. K. Perkins, Nano Letters 6 8 1747-1751 **(2006)**

[9] K.G. Ong, K. Zeng, C.A. Grimes, *IEEE Sensors Journal*, 2, p. 82 **(2002)**

[10] Y. Lin, F. Lu, J. Wang, *Electroanalysis*, 16, p.145 **(2004)**; S. Sotiropoulou, N. A. Chaniotakis, *Analytical and Bioanalytical Chemistry*, 375, p.103 **(2003)**; J. Wang *Electroanalysis*, 17, p. 7 **(2004)**

[11] D. Cai, J.M. Mataraza, Z.H. Qin, Z. Huang, J. Huang, T.C. Chiles, D. Carnahan, K. Kempa, Z. Ren, *Nature Methods*, 2, p. 449 **(2005)**

[12] R. Singh, D. Pantarotto, D. McCarthy, O. Chaloin, J. Hoebeke, C.D. Partidos, J.P. Briand, M. Prato, A. Bianco, K. Kostarelos, *J. Am. Chem. Soc.*, 127, p. 4388 **(2005)**

[13] K.H. Park, M. Chhowalla, Z. Iqbal, F. Sesti, *J. of Bio. Chem.*, 278, p. 50212 **(2003)**

[14] *"Understanding Carbon Nanotubes: From Basics to Applications"*, Series: Lecture Notes in Physics, Vol. 677, ISBN: 3-540-26922-3, A. Loiseau, P. Launois, P. Petit, S. Roche, J.–P. Salvetat (Eds.), Springer **(2006)**]

[15] S. Reich, C. Thomsen, J. Maultzsch, "Carbon Nanotubes: Basic Concepts and Physical Properties", ISBN3-527-40386-8, Wiley-VCH, Berlin (2004)

[16] R. Saito, G. Dresselhaus, M.S. Dresselhaus, *Physical Properties of Carbon Nanotubes*, Imperial College Press (London, 1998)].

[17] L. A. Girifalco, M. Hodak, R. S. Lee, Phys. Rev. B **62** 13104 **(2000)**

[18] B. Yakobson, L. Couchman, J. Nanoparticle Research 8 1 105-110(6) **(2006)**

[19] J. –C. Charlier, X. Gonze, J. –P. Michenaud, Europhys. Lett., 28 403 **(1994).**

[20] M. C. Schabel, J. L. Martins, Phys. Rev. B 46 7185 **(1992)**

[21] L. X. Zheng, M. J. O'Connell, S. K. Doorn, X. Z. Liao, Y. H. Zhao, E. A. Akhadov, M. A. Hoffbauer, B. J. Roop, Q. X. Jia, R. C. Dye, D. E. Peterson, S. M. Huang, J. Liu, Y. T. Zhu, Nat Materials 3 673 **(2004)**

[22] J. W. Mintmire, C. T. White in *"Carbon Nanotubes – Preparation and Properties"*, Ed. T. W. Ebbesen, CRC Press (Boca Raton, 1997), p.191-209.

[23] picture taken from homepage of R.E. Smalley at Rice University, USA: http://cnst.rice.edu/smalleygroup/res.htm.

[24] J. W. G. Wildöer, L. C. Venema, A. G. Rinzler, R. E. Smalley, C. Dekker, Nature 391, 59 **(1998)**.

[25] N. D. Lang in *"Scanning Tunneling Microscopy III"*, Ed R. Wiesendanger and H. –J. Güntherodt, Springer Series in Surface Sciences 29, Springer Verlag (Berlin, Heidelberg, New York 1993), p.7-21.

[26] K.G. Ong, K. Zeng, C.A. Grimes, *IEEE Sensors Journal*, 2, p. 82 **(2002)**

[27] S. Heinze, J. Tersoff, Ph. Avouris, *Lect. Notes Phys.*, 680, p. 381 **(2005)**

[28] C.H. Ke, N. Pugno, B. Peng, H.D. Espinosa, *J. Mech. Phys. Solids*, 53, p. 1314 **(2005)**;

[29] A. M. Fennimore, T. D. Yuzvinsky, W.-Q. Han, M. S. Fuhrer, J. Cumings, A. Zettl, *Nature*, 424, p. 408 **(2003)**

[30] S.W. Lee, D.S. Lee, R.E. Morjan, S.H. Jhang, M. Sveningsson, O.A. Nerushev, Y.W. Park, E.E.B. Campbell, *Nano Lett.*, 4, p. 2047 **(2004)**

[31] A. Javey, J. Guo, D. B. Farmer, Q. Wang, D. Wang, R. G. Gordon, M. Lundstrom, H. Dai, *Nano Lett.*, 4, p. 447 **(2004)**

[32] Q. Zheng, Q. Jiang, Phys Rev Lett 88 4 045503 **(2002).**

[33] M. Radosavljevic, M. Freitag, K.V. Thadani, A.T. Johnson, *Nano Lett.* 2, p. 761 **(2002)**

[34] P.G. Collins, K. Bradley, M. Ishigami, A. Zettl, *Science* 287 1801 **2000**

[35] D. Kang, N. Park, J. Ko, E. Bae, W. Park, *Nanotechnology* 16 1048-1052 **(2005)**

[36] V. Derycke, R. Martel, J. Appenzeller, Ph. Avouris, *Nano Lett.* 1, 453 **(2001)**]

[37] V. Derycke, R. Martel, J. Appenzeller, Ph. Avouris, *Nano Lett.* 1, 453 **(2001)**]

[38] M. Bockrath, D. Cobden, P. McEuen, N. Chopra, A. Zettl, A; Thess, R. Smalley, Science 275, 1922-1925 **(1997)**.

[39] J. Nygard, D. H. Cobden, M. Bockrath, P. L. McEuen, P. E. Lindelof, Appl. Phys. A 69 297-304 **(1999)**

[40] T. Tombler, C. Zhou, J. Kong, H. Dai, Appl. Phys. Lett. 76 2412 **(2000).**

[41] T. Tombler, C. Zhou, L. Alexeyev, J. Kong, H. Dai, L. Liu, C. Jayanthi, M. Tang, S. Wu, Nature 405 769 **(2000).**

[42] H. Dai, J. Kong, C. Zhou, N. Franklin, T. Tombler, A. Cassell, S. Fan, M. Chapline, J. Phys.Chem. 103 11246-11255 **(1999)**

[43] H. Dai, Physics World 13, 43-47 **(2000)**

[44] H. Soh et al, Appl. Phys. Lett. 75, 627-629 (1999)

[45] J.Kong, N. Franklin, C. Zhou, M. Chapline, S. Peng, K. Cho, H. Dai, Science 287, 622-625 **(2000)**

[46] A. Cassell, N. Franklin, T. Tombler, E. Chan, J. Han, H. Dai, J. Am. Chem. Soc. 121 7975-7976 **(1999)**

[47] N. Franklin, H. Dai, *Adv. Mater.* 12 890 **(2000)**

[48] A. Ismach, L. Segev, E. Wachtel, E. Joselevich, Angew. Chem. Int. Ed. 43, 6140, **(2004)**

[49] A. Ismach, D. Kantorovich, E. Joselevich, J. Am. Chem. Soc. 127, 11554, **(2005)**

[50] P. Avouris; J. Appenzeller; R. Martel; S. Wind. *J. Proc. IEEE*, 91, 1772-1784, **(2003)**.

[51] M. S. Fuhrer; B. M. Kim; T. Dürkop; T. Brintlinger. *Nano Lett.*, 2, 755-759, **(2002)**

[52] A. Javey; J. Guo; Q. Wang; M. Lundstrom; H. Dai. *Nature*, 424, 654-657, **(2003)**

[53] P. G. Collins; M. S. Arnold; P. Avouris. *Science*, 292, 706-709, **(2001)**.

[54] K. Balasubramanian; R. Sordan; M. Burghard; K. Kern. *Nano Lett.*, *4*, 5, 1353-1355, **(2004)**.

[55] K. Balasubramanian; M. Friedrich; C. Jiang; Y. Fan; A. Mews; M. Burghard; K. Kern. *Adv. Mater. (Weinheim, Ger.)*, 15, 1515-1518, **(2003)**

[56] C. Menard-Moyon, N. Izard, E. Doris, C. Mioskowski, JACS 128 (20), 6552 **(2006)**

[57] M. Arnold, A. Green, J. Hulvat, S. Stupp, M. Hersam, Nature Nanotechnology 1 60 **(2006).**

[58] R. Krupke, F. Hennrich, H. v. Löhneysen, M. M. Kappes*, Science*, 301(5631), 344 **(2003)**

[59] H. Peng, N. T. Alvarez, C. Kittrell, R. H. Hauge, H. K. Schmidt, *J. Am. Chem. Soc.*, 128 (26), 8396 - 8397, **(2006)**: http://pubs.acs.org/cgi-bin/abstract.cgi/jacsat/2006/128/i26/abs/ja0621501.html]

[60] C. Ducati, K. Koziol, S. Friedrichs, T. J. V. Yates, M. Shaffer, P. Midgley, A. Windle, Small 2 6 74-784 **(2006)**

[61] S. Heinze, J. Tersoff, Ph. Avouris, *Lect. Notes Phys.*, 680, p. 381 **(2005)**

[62] S. Heinze, J. Tersoff, R. Martel, V. Derycke, J. Appenzeller, Ph. Avouris*, Phys. Rev. Lett.*, 89, 106801 **(2002)**

[63] S. Heinze, M. Radosavljevic, J. Tersoff, Ph. Avouris, *Phys. Rev B*, 68, 235418 **(2003)**

[64] A. Javey, J. Guo, D.B. Farmer, Q. Wang, D. Wang, R.G. Gordon, M. Lundstrom, H. Dai, *Nano Lett.*, 4, p. 447 **(2004)**

[65] O.T. Heyning, P. Bernier, M. Glerup, *Chem. Phys. Lett.* 409 43–47 **(2005)**

[66] B.C. Satishkumar, P. John Thomas, A. Govindaraj, C.N.R. Rao, *APL* 77 (16) 2530 **(2000)**

[67] F.L. Deepak, A. Govindaraj, C.N.R. Rao, *Chem. Phys. Lett.* 345, 5 **(2001)**

[68] J. Li, C. Papadopoulos, and J. Xu. *Nature* **402**, 253(1999)

[69] C. Papadopoulos, A. Rakitin, J. Li, A. S. Vedeneev, J. M. Xu, PRL **85**, p. 3476 (2000)

[70] C. Papadopoulos, A. J. Yin, J. M. Xu, Applied Physics Letters 85, p. 1769 (2004)

[71] W. Z. Li, J. G. Wen, and Z. F. Ren, Applied Physics Letters 79, p. 1879 (2001)

[72] M. Menon, A. N. Andriotis, D. Srivastava, I. Ponomareva, L. A. Chernozatonskii, PRL **91**, 145501 (2003)

[73] C. P. Ewels, M. Glerup, V. Krystic, ”Nitrogen and Boron Doping in Carbon Nanotubes”, to appear in ”Chemistry of Carbon Nanotubes”, ed. V Basiuk, American Scientific Press (2007).

[74] Y. Chen; R.C. Haddon; S. Fang; A.M. Rao; P.C. Eklund; W.H. Lee; E.C. Dickey; E.A. Grulke; J.C. Pendergrass; A. Chavan; B.E. Haley; R.E. Smalley. *J. Mater. Res.*, *13*, 9, 2423-2431, **(1998)**

[75] S. Niyogi; M. A. Hamon; H. Hu; B. Zhao; P. Bhomik; R. Sen; M. E. Itkis; R. C. Haddon. *Acc. Chem. Res.*, 35, 1105-1113, **(2002)**

[76] J. L. Bahr; J. M. Tour. *J. Mater. Chem.*, 12, 1952-1958, **(2002)**

[77] A. Hirsch. *Angew. Chem. Int. Ed*, *41*, 11, 1853-1859, **(2002)**

[78] S. Banerjee; M. G. C. Kahn; S. S. Wong. *J. Chem. Eur.*, 9, 1898 -1908, **(2003)**

[79] C. A. Dyke; J. M. Tour. *J. Phys. Chem. A*, *108*, 51, **(2004)**

[80] S. Banerjee; T. Hemraj-Benny; S. S. Wong. *Adv. Mater. (Weinheim, Ger.)*, *17*, 1, 17 - 29, **(2005)**

[81] K. Balasubramanian; M. Burghard. *Small*, *1*, 2, 180 -192, **(2005)**.

[82] M. A. Hamon; M. E. Itkis; S. Niyogi; T. Alvaraez; C. Kuper; M. Menon; R. C. Haddon. *J. Am. Chem. Soc.*, *123*, 11292-11293, **(2001)**

[83] R. C. Haddon, *Science*, 261, 1545-1550, **(1993)**

[84] R. C. Haddon, *J. Am. Chem. Soc.*, 112, 3385-3389, (**1990**).

[85] P. W. Rabideau; A. Sygula, *Acc. Chem. Res.*, 29, 235-242, (**1996**)

[86] L. T. Scott; M. S. Bratcher; S. Hagen. *J. Am. Chem. Soc.*, 118, 8743-8744, (**1996**)

[87] R. C. Haddon; K. Raghavachari. *Tetrahedron*, 52, 5207-5220, (**1996**)

[88] B. R. Weedon; R. C. Haddon; H. P. Spielmann; M. S. Meier. *J. Am. Chem. Soc.*, 121, 335-340, (**1999**)

[89] G.J. Bodwell; J.N. Bridson; T.J. Houghton; J.W.J. Kennedy; M.R. Mannion. *Chem. Eur. J.*, 5, 1823-1827, (**1999**)

[90] D. Srivastava; D.W. Brenner; J.D. Schall; K.D. Ausman; M.Yu; R.S. Ruoff. *J. Phys. Chem. B*, 103, 4330-4337, (**1999**)

[91] Z. Chen; W. Thiel; A. Hirsch. *Chem. Phys. Chem.* 4, 93-97, (**2003**)

[92] Z. Chen; S. Nagase; A. Hirsch; R.C. Haddon; W. Thiel; P.v.R. Schleyer. *Angew. Chem. Int. Ed*, 116, 1578-1580, (**2004**)

[93] M. Holzinger; A. Hirsch; F. Hennrich; M. M. Kappes; A. Dziakowa; L. Ley; R. Graupner. *AIP Conf. Proc.*, *633*, 1, 96, (**2002**).

[94] H. Hiura; T.W. Ebbesen; K. Tanigaki. *Adv. Mater*, 7, 275, (**1995**).

[95] T.W. Ebbesen; H. Hiura; M. E. Bisher; M.M.J. Treacy; J.L. Shreeve-Keyer; R.C. Haushaiter. *Adv. Mater*, *8*, 155, (**1996**)

[96] J. Chen; M.A. Hamon; H. Hu; Y. Chen; A.M. Rao; P.C. Eklund; R.C. Haddon. *Science (Washington, D. C.)*, *282*, 5386, 95-98, (**1998**)

[97] J. Liu; A.G. Rinzler; H. Dai; J.H. Hafner; R.K. Bradley; P.J. Boul; A. Lu; T. Iverson; K. Shelimov; C.B. Huffman; F. Rodriguez-Macias; Y.-S. Shon; T.R. Lee; D.T. Colbert; R.E. Smalley. *Science (Washington, D. C.)*, *280*, 5367, 1253-1256, (**1998**)

[98] D.B. Mawhinney; V. Naumenko; A. Kuznetsova; J. John T. Yates; J. Liu; R.E. Smalley. *J. Am. Chem. Soc.*, 122, 2383-2384, (**2000**).

[99] A. Kuznetsova; D.B. Mawhinney; V. Naumenko; J.T.Y. Jr.; J. Liu; R.E. Smalley. *Chem. Phys. Lett.*, *321*, 3-4, 292-296, (**2000**).

[100] P.M. Ajayan; T.W. Ebbesen; T. Ichihashi; S. Iijima; K. Tanigaki; H. Hiura. *Nature*, 361, 333, (**1993**).

[101] M. Holzinger; O. Vostrowsky; A. Hirsch; F. Hennrich; M. Kappes; R. Weiss; F. Jellen. *Angew. Chem., Int. Ed.*, *40*, 21, 4002-4005, (**2001**)

[102] H. Peng; P. Reverdy; V.N. Khabashesku; J.L. Margrave; *Chem. Commun.*, 362-363, (**2003**).

[103] H.S. Chen; A.R. Kortan; R.C. Haddon; N.J. Kopylov. *J. Phys. Chem. B*, 97, 3088-3090, (**1993**)

[104] M. Holzinger; J. Abraham; P. Whelan; R. Graupner; L. Ley; F. Hennrich; M. Kappes; A. Hirsch. *J. Am. Chem. Soc.*, *28*, 125, 8566-8580, (**2003**)

[105] V. Georgakilas; K. Kordatos; M. Prato; D. M. Guldi; M. Holzinger; A. Hirsch. *J. Am. Chem. Soc.*, *124*, 5, 760, (**2002**)

[106] G. Viswanathan; N. Chakrapani; H. Yang; B. Wei; H. Chung; K. Cho; C. Y. Ryu; P. M. Ajayan. *J. Am. Chem. Soc.*, 125, 9258-9259, (**2003**)

[107] R. Blake; Y.K. Gun'ko; J.N. Coleman; M. Cadek; A. Fonseca; J.B. Nagy; W.J. Blau. *J. Am. Chem. Soc.*, 126, 10226-10227, (**2004**).

[108] S. Chen; W. Shen; G. Wu; D. Chen; M. Jiang. *Chem. Phys. Lett.*, 402, 312-317, (**2005**)

[109] R. Graupner; J. Abraham; D. Wunderlich; A. Vencelová; P. Lauffer; J. Röhrl; M. Hundhausen; L. Ley; A. Hirsch. *J. Am. Chem. Soc.*, *128*, 20, 6683-6689, (**2006**)

[110] E.T. Mickelson; C.B. Huffman; A.G. Rinzler; R.E. Smalley; R.H. Hauge; J.L. Margrave. *Chem. Phys. Lett.*, 296, 188-194, (**1998**)

[111] J.L. Bahr; J. Yang; D.V. Kosynkin; M.J. Bronikowski; R.E. Smalley; J. M. Tour. *J. Am. Chem. Soc.*, 123, 6536-6542, (**2001**)

[112] J.L. Bahr; J.M. Tour. *Chem. Mater.*, 13, 3823-3824, (**2001**).

[113] M. Holzinger; J. Steinmetz; S. Roth; M. Glerup; R. Graupner. *AIP Conf. Proc.*, *786*, 211, (**2005**).

[114] M.J. O'Connell; S.M. Bachilo; C.B. Huffman; V.C. Moore; M.S. Strano; E.H. Haroz; K.L. Rialon; P.J. Boul; W.H. Noon; C. Kittrell; J. Ma; R.H. Hauge; R.B. Weisman; R.E. Smalley. *Science*, 297, 593, (**2002**)

[115] C.A. Dyke; J.M. Tour. *Nano Lett.*, 3, 1215, (**2003**)

[116] F. Liang; A.K. Sadana; A. Peera; J. Chattopadhyay; Z. Gu; R.H. Hauge; W.E. Billups. *Nano Lett.*, 4, 1257-1260, (**2004**).

[117] J. Chattopadhyay; A.K. Sadana; F. Liang; J.M. Beach; Y. Xiao; R.H. Hauge; W.E. Billups. *Org. Lett.*, 7, 4067-4069, (**2005**)

[118] M.A. Hamon; J. Chen; H. Hu; Y. Chen; M.E. Itkis; A.M. Rao; P.C. Eklund; R.C. Haddon. *Adv. Mater. (Weinheim, Ger.)*, *11*, 10, 834-840, (**1999**)

[119] J. Chen; A.M. Rao; S. Lyuksyutov; M. E. Itkis; M.A. Hamon; H. Hu; R.W. Cohn; P.C. Eklund; D.T. Colbert; R.E. Smalley; R.C. Haddon. *J. Phys. Chem. B*, *105*, 13, 2525-2528, (**2001**)

[120] R.C. Haddon; J. Chen. *USA, (Patent,* University of Kentucky Research Foundation, USA). Patent Number 6187823, 8, (**2001**)

[121] B. Neises; W. Steglich. *Angew. Chem. Int. Ed.*, 17, 522-524, (**1978**)

[122] S.S. Wong; A.T. Woolley; E. Joselevich; C.L. Cheung; C.M. Lieber. *J. Am. Chem. Soc.*, 120, 8557-8558, (**1998**).

[123] M. Holzinger; A. Hirsch; M. Burghard; P. Bernier. *AIP Conf. Proc.*, 544(1), 246, (**2000**)

[124] M.C. Desai; L.M.S. Stramiello. *Tetrahedron Lett.*, *34*, 48, 7685, (**1993**)

[125] H. Kohasaka; D.A. Carson. *Journal of Clinical Laboratory Analysis*, 8, 452, (**1994**)

[126] K.A. Williams; P.T.M. Veenhuizen; B.G. d. l. Torre; R. Eritja; C. Dekker. *Nature*, 420, 761, (**2002**)

[127] M. Holzinger; J. Steinmetz; D. Samaille; M. Glerup; M. Paillet; P. Bernier; L. Ley; R. Graupner. *Carbon*, 42, 941-947, (**2004**)

[128] R. Weiss; S. Reichel; M. Handke; F. Hampel. *Angew. Chem. Int. Ed*, *37*, 344, (**1998**).

[129] S. Reichel. University of Erlangen-Nürnberg, PhD (**1998**)

[130] R. Weiss; S. Reichel. *Eur. J. Inorg. Chem*, 1935, (**2000**)

[131] I.C. Calder; T.M. Spotswood; W.H.F. Sasse. *Tetrahedron Lett.*, 65, (**1963**)

[132] P.J.Fagan; P. J. Krusic; C.N. McEwen; J. Lazar; D.H. Parker; N. Herron; E. Wasserman. *Science*, 262, 404., (**1993**)

[133] M.S.P. Shaffer; K. Koziol. *Chem. Commun.*, 2074-2075, (**2002**)

[134] Y. Ying; R.K. Saini; F. Liang; A.K. Sadana; W.E. Bulleps. *Organic Letters*, 5, 1471-1473, (**2003**)

[135] H. Xia; Q. Wang; G. Qiu. *Chem. Mater.*, 15, 3879-3886, (**2003**)

[136] C.B. Wooster; K. L. Godfrey. *J. Am. Chem. Soc.*, 59, 596, (**1937**)

[137] A. Birch. *J. Quart. Rev.*, 4, 69, (**1950**)

[138] J. Abraham. University of Erlangen-Nürnberg, Ph. D., (**2005**)

[139] P. Petit; C. Mathis; C. Journet; P. Bernier. *Chem. Phys. Lett.*, 305, 370-374, (**1999**)

[140] C. Mathis; B. François. *Synth. Met.*, 9, 347, (**1984**)

[141] A. Pénicaud; P. Poulin; A. Derré; E. Anglaret; P. Petit. *J. Am. Chem. Soc.*, 127, 8-9, (**2004**)

[142] A. Hirsch; M. Brettreich. *Fullerenes: Chemistry and Reaction*, Wiley-VCH: Weinheim **2005**

[143] M. Maggini; G. Scorrano; M. Prato. *J. Am. Chem. Soc.*, 115, 9798-9799, (**1993**)

[144] M. Prato; M. Maggini. *Acc. Chem. Res.*, 31, 519-526, (**1998**).

[145] D. Pantorotto; C. D. Partidos; R. Graff; J. Hoebke; J.-P. Briand; M. Prato; A. Bianco. *J.Am.Chem.Soc.*, 125, 6160, (**2003**)

[146] D. M. Guldi; M. Marcaccio; D. Paolucci; F. Paolucci; N. Tagmatarchis; D. Tasis; E. Vazquez; M. Prato. *Angew. Chem. Int. Ed.*, 42, 4206, (**2003**)

[147] D. Pantarotto; R. Singh; D. McCarthy; M. Erhardt; J.-P. Briand; M. Prato; K. Kostarelos; A. Bianco. *Angew. Chem., Int. Ed.*, 43, 5242- 5246, (**2004**)

[148] N. Tagmatarchis; M. Prato. *J. Mater. Chem.*, 14, 437-439, (**2004**)

[149] M. Delamar; G. Désarmot; O. Fagebaume; R. Hitmi; J. Pinson; J.-M. Savéant. *Carbon*, 35, 801-807, (**1997**)

[150] P. Allongue; M. Delamar; B. Desbat; O. Fagebaume; R. Hitmi; J. Pinson; J.-M. Savéant. *J. Am Chem. Soc.*, 119, 201-207, (**1997**)

[151] B. Ortiz; C. Saby; G. Y. Champagne; D. J. Bélanger. *Electroanal. Chem.*, 455, 75-81, (**1998**)

[152] C. Saby; B. Ortiz; G. Y. Champagne; D. Bélanger. *Langmuir*, 13, 6805-6813, (**1997**)

[153] M. Delamar; R. Hitmi; J. Pinson; J. M. Savéant. *J. Am. Chem. Soc.*, 114, 5883-5884, (**1992**)

[154] J. K. Kariuki; M. T. McDermott. *Langmuir*, 15, 6534-6540, (**1999**)

[155] S.E. Kooi; U. Schlecht; M. Burghard; K. Kern. *Angew. Chem. Int. Ed.*, 41, 1353-1355, (**2002**)

[156] M. Glerup; J. Steinmetz; D. Samaille; O. Stéphane; S. Enouz; A. Loiseau; S. Roth; P. Bernier. *Chem. Phys. Lett.*, 387, 193, (**2004**)

[157] A.H. Nevidomskyy; G. Csányi; M.C. Payne. *Phys. Rev. Lett.*, 91, 105502, (**2003**)

[158] F. Hauke; A. Hirsch. *J. Chem. Soc. Chem. Commun.*, 21, 2199, (**1999**)

[159] V.N. Khabashesku, W.E. Billups, J.L. Margrave, '*Fluorination of single-wall carbon nanotubes and subsequent derivatization reactions', Accounts of Chemical Research*, 35, 1087 (**2002**)

[160] H.F. Bettinger, '*Experimental and computational investigations of the properties of fluorinated single-walled carbon nanotubes',* Chem Phys Chem, 4, 1283 (**2003**)

[161] T. Nakajima, S. Kasamatsu, Y. Matsuo, '*Synthesis and characterization of fluorinated carbon nanotube', European Journal of Solid State and Inorganic Chemistry*, 33, 831 (**1996**)

162 E.T. Mickelson, C.B. Huffman, A.G. Rinzler, R.E. Smalley, R.H. Hauge, J.L. Margrave, *Fluorination of single-wall carbon nanotubes, Chemical Physics Letters*, 296, 188 **(1998)**

163 E.T. Mickelson, I.W. Chiang, J.L. Zimmerman, P.J. Boul, J. Lozano, J. Liu, R.E. Smalley, R.H. Hauge, J.L. Margrave, *Solvation of fluorinated single-wall carbon nanotubes in alcohol solvents, Journal of Physical Chemistry B*, 103, 4318 **(1999)**

164 K.N. Kudin, H.F. Bettinger, G.E. Scuseria, *Fluorinated single-wall carbon nanotubes, Physical Review B: Condensed Matter and Materials Physics,* 63, 045413/1-13/8 **(2001)**

165 P.J. Boul, J. Liu, E.T. Mickelson, C.B. Huffman, L.M. Ericson, I.W. Chiang, K.A. Smith, D.T. Colbert, R.H. Hauge, J.L. Margrave, R.E. Smalley, *Reversible sidewall functionalization of buckytubes,* Chemical Physics Letters 310 (1999) 367-72

166 K.F. Kelly, I.W. Chiang, E.T. Mickelson, R.H. Hauge, J.L. Margrave, X. Wang, G.E. Scuseria, C. Radloff, N.J. Halas, *Insight into the mechanism of sidewall functionalization of single-walled nanotubes: an STM study,* Chemical Physics Letters 313 (1999) 445-50

167 R.K. Saini, I.W. Chiang, H. Peng, R.E. Smalley, W.E. Billups, R.H. Hauge, J.L. Margrave, *Covalent Sidewall Functionalization of Single Wall Carbon Nanotubes,* Journal of the American Chemical Society 125 (2003) 3617-21.

168 J.L. Stevens, A.Y. Huang, H. Peng, I.W. Chiang, V.N. Khabashesku, J.L. Margrave, Nano Letters 3 (2003) 331-36

169 L. Valentini, D. Puglia, I. Armentano, J.M. Kenny, *Sidewall functionalization of single-walled carbon nanotubes through CF4 plasma treatment and subsequent reaction with aliphatic amines,* Chemical Physics Letters 403 (2005) 385-89

170 U. Dettlaff-Weglikowska, V. Skakalova, J. Meyer, J. Cech, B.G. Mueller, S. Roth, *Effect of fluorination on electrical properties of single walled carbon nanotubes and C60 peapods in networks,* Current Applied Physics 7 (1), p.42-46 (2006)

171 G. Seifert, T. Kohler, T. Frauenheim, *Molecular wires, solenoids, and capacitors by sidewall functionalization of carbon nanotubes,* Applied Physics Letters 77 (2000) 1313-15.

172 A. Hamwi, P. Gendraud, H. Gaucher, S. Bonnamy, F. Beguin, *Electrochemical properties of carbon nanotube fluorides in a lithium cell system,* Molecular Crystals and Liquid Crystals Science and Technology, Section A: Molecular Crystals and Liquid Crystals 310 (1998) 185-90

173 I. Mukhopadhyay, Y. Yokoyama, F. Okino, S. Kawasaki, H. Touhara, W.K. Hsu, *Effect of chemical modification on electrochemical Li insertion in highly ordered multi-wall carbon nanotubes,* Proceedings - Electrochemical Society 2001-14 (2001) 37-40.

174 H. Peng, Z. Gu, J. Yang, J.L. Zimmerman, P.A. Willis, M.J. Bronikowski, R.E. Smalley, R.H. Hauge, J.L. Margrave, *Fluorotubes as Cathodes in Lithium Electrochemical Cells,* Nano Letters 1 (2001) 625-29

175 M.J. Root, *Comparison of Fluorofullerenes with Carbon Monofluorides and Fluorinated Carbon Single Wall Nanotubes: Thermodynamics and Electrochemistry,* Nano Letters 2 (2002) 541-43

176 J.Y. Lee, K.H. An, J.K. Heo, Y.H. Lee, *Supercapacitors using fluorinated singlewalled carbon nanotube,* Proceedings - Electrochemical Society 2003-15 (2003) 366-70.

177 J.Y. Lee, K.H. An, J.K. Heo, Y.H. Lee, *Fabrication of Supercapacitor Electrodes Using Fluorinated Single-Walled Carbon Nanotubes,* Journal of Physical Chemistry B 107 (2003) 8812-15.

178 T. Hayashi, M. Terrones, C. Scheu, Y.A. Kim, M. Ruehle, T. Nakajima, M. Endo, *NanoTeflons: Structure and EELS Characterization of Fluorinated Carbon Nanotubes and Nanofibers,* Nano Letters 2 (2002) 491-96

179 V. Gupta, *Comments on \"NanoTeflons: Structure and EELS Characterization of Fluorinated Carbon Nanotubes and Nanofibers\",* Nano Letters 4 (2004) 999

180 T. Hayashi, *Reply to \"A Comment on 'NanoTeflons: Structure and EELS Characterization of Fluorinated Carbon Nanotubes and Nanofibers'\",* Nano Letters 4 (2004) 1001-02

181 V.N. Khabashesku, J.L. Margrave, E.V. Barrera, *Functionalized carbon nanotubes and nanodiamonds for engineering and biomedical applications,* Diamond and Related Materials 14 (2005) 859-66

182 F.J. Owens, *Raman and mechanical properties measurements of single walled carbon nanotube composites of polyisobutylene,* Journal of Materials Chemistry 16 (2006) 505-08

183 P.R. Marcoux, J. Schreiber, P. Batail, S. Lefrant, J. Renouard, G. Jacob, D. Albertini, J.-Y. Mevellec, *A spectroscopic study of the fluorination and defluorination reactions on single-walled carbon nanotubes,* Physical Chemistry Chemical Physics 4 (2002) 2278-85

184 B.N. Khare, P. Wilhite, M. Meyyappan, *The fluorination of single wall carbon nanotubes using microwave plasma,* Nanotechnology 15 (2004) 1650-54

[185] A. Felten, C. Bittencourt, J.J. Pireaux, G. Van Lier, J.C. Charlier, *Radio-frequency plasma functionalization of carbon nanotubes surface O2, NH3, and CF4 treatments,* Journal of Applied Physics 98 (2005) 074308/1-08/9

[186] N.F. Yudanov, A.V. Okotrub, Y.V. Shubin, L.I. Yudanova, L.G. Bulusheva, A.L. Chuvilin, J.-M. Bonard, *Fluorination of Arc-Produced Carbon Material Containing Multiwall Nanotubes,* Chemistry of Materials 14 (2002) 1472-76

[187] A.V. Okotrub, N. Maksimova, T.A. Duda, A.G. Kudashov, Y.V. Shubin, D.S. Su, E.M. Pazhetnov, A.I. Boronin, L.G. Bulusheva, *Fluorination of CNx Nanotubes,* Fullerenes, Nanotubes, and Carbon Nanostructures 12 (2004) 99-104

[188] P.N. Gevko, L.G. Bulusheva, A.V. Okotrub, N.F. Yudanov, I.V. Yushina, K.A. Grachev, A.M. Pugachev, N.V. Surovtsev, E. Flahaut, *Optical absorption and raman spectroscopy study of the fluorinated double-wall carbon nanotubes,* Fullerenes, Nanotubes, and Carbon Nanostructures 14 (2006) 233-38

[189] E. Unger, M. Liebau, G.S. Duesberg, A.P. Graham, F. Kreupl, R. Seidel, W. Hoenlein, *Fluorination of carbon nanotubes with xenon difluoride,* Chemical Physics Letters 399 (2004) 280-83.

[190] K.H. An, J.G. Heo, K.G. Jeon, D.J. Bae, C. Jo, C.W. Yang, C.-Y. Park, Y.H. Lee, Y.S. Lee, Y.S. Chung, *X-ray photoemission spectroscopy study of fluorinated single-walled carbon nanotubes,* Applied Physics Letters 80 (2002) 4235-37

[191] Y.S. Lee, T.H. Cho, B.K. Lee, J.S. Rho, K.H. An, Y.H. Lee, *Surface properties of fluorinated single-walled carbon nanotubes,* Journal of Fluorine Chemistry 120 (2003) 99-104.

[192] A. Hamwi, H. Alvergnat, S. Bonnamy, F. Beguin, *Fluorination of carbon nanotubes,* Carbon 35 (1997) 723-28

[193] C.P. Ewels, G. Van Lier, J.-C. Charlier, M.I. Heggie, P.R. Briddon, *Pattern Formation on Carbon Nanotube Surfaces,* Physical Review Letters 96 (2006) 216103/1-03/4

[194] C.W. Bauschlicher, *Hydrogen and fluorine binding to the sidewalls of a (10,0) carbon nanotube,* Chemical Physics Letters 322 (2000) 237-41

[195] R.L. Jaffe, *Quantum Chemistry Study of Fullerene and Carbon Nanotube Fluorination,* Journal of Physical Chemistry B 107 (2003) 10378-88

[196] G. Van Lier, C.P. Ewels, F. Zuliani, A. De Vita, J.-C. Charlier, *Theoretical Analysis of Fluorine Addition to Single-Walled Carbon Nanotubes: Functionalization Routes and Addition Patterns,* Journal of Physical Chemistry B 109 (2005) 6153-58

[197] W. Zhao, C. Song, B. Zheng, J. Liu, T. Viswanathan, *Thermal Recovery Behavior of Fluorinated Single-Walled Carbon Nanotubes,* Journal of Physical Chemistry B 106 (2002) 293-96.

[198] M. L. Shofner, V.N. Khabashesku, E.V. Barrera, *Processing and Mechanical Properties of Fluorinated Single-Wall Carbon Nanotube-Polyethylene Composites,* Chemistry of Materials 18 (2006) 906-13

[199] A. Bachtold, M.S. Fuhrer, S. Plyasunov, M. Forero, E.H. Anderson, A. Zettl, P.L. McEuen, *Phys. Rev. Lett.* 84, 6082 **(2000)**

[200] V. Krstić, S. Roth, M. Burghard, *Phys. Rev. B* 62, p. R16353, **(2000)**

[201] M.S. Fuhrer, M. Forero, A. Zettl, P.L. McEuen in *Electronic Properties of Molecular Materials*, ed. by H. Kuzmany, J. Fink, M. Mehring, S. Roth, AIP **59**1, New York, p. 401-404 (2001).

[202] R. Egger, A. Bachtold, M.S. Fuhrer, M. Bockrath, D.H. Cobden and P.L. McEuen in *Interacting electrons in Nanostructures*, ed. by R. Haug and H. Schoeller, Lecture Notes in Physics 579, Springer-Verlag (Berlin, Heidelberg, New York, 2001).

[203] R. Saito, G. Dresselhaus, M.S. Dresselhaus, *Physical Properties of Carbon Nanotubes*, Imperial College Press (London, 1998), p. 17-33

[204] T. Hertel and G. Moos, *Phys. Rev. Lett.* 84, 5002 **(2000)**

[205] C.L. Kane, M.P.A. Fisher, *Phys. Rev.* B 68, 15233 **(1992);** C.L. Kane, M.P.A. Fisher, *Phys. Rev. Le*tt. **6**8, p. 1220 **(1992)**

[206] F.D.M. Haldane, *Phys. Rev. Lett.* **47**, p. 1840 (1981).

[207] S. Sanvito, Y.K. Kwon, D. Tomanek, C.J. Lambert, *Phys. Rev. Lett.* 84, 1974 **(2000)**

[208] V.H. Crespi, M.L. Cohen, A. Rubio, *Phys. Rev. Lett.* 79, 2093 **(1997)**

[209] S. Roche, F. Triozon, A. Rubio, D. Mayou, *Phys. Lett.* A 285, p. 94 **(2001)**

[210] S. Frank, P. Poncharal, Z.L. Wang and W.A. de Heer, *Science* 280, p. 1744 **(1998)**

[211] A. Bachtold, C. Strunk, J.-P. Salvetat, J.-M. Bonard, L. Forró, T. Nussbaumer, C. Schönenberger, *Nature* **397**, p. 673 **(1999)**

[212] C. Schönenberger, A. Bachtold, C. Strunk, J.P. Salvetat, L. Forró, *Appl. Phys. A: Mater. Sci. Process.* **69**, p. 283 (1999); A. Bachtold, M. de Jonge, K. Grove-Rasmussen, P. L. McEuen, M. Buitelaar, C. Schönenberger, *Phys. Rev. Lett.* 87, 166801 **(2001)**

[213] E. G. Mishchenko, A. V. Andreev, L. I. Glazman, *Phys. Rev. Lett.* 87, 246801 **(2001)**

[214] V. Krstić, S. Blumentritt, J. Muster, S. Roth, A. Rubio, *Phys. Rev. B* 67, 041401(R) **(2000)**

[215] A.H. Nevidomskyy, G. Csanyi, M.C. Payne, *Phys. Rev. Lett.* 91, 105502 **(2003)**

[216] H.S. Kang , S. Jeong, *Phys. Rev.* B 70, 233411 **(2004)**

[217] M.F.Lin, D.S. Chuu, *Phys. Rev.* B 56, p. 4996 **(1997)**

[218] M. Büttiker, *Phys. Rev. Lett.* **57**, p. 1761 (1986). M. Büttiker, *IBM J. R. Develop* **32**, p. 317 **(1988)** M. Büttiker, *Phys. Rev.* B **33**, p. 3020 (1986). For an review on this topic see also S. Datta, *Electronic Transport in Mesoscopic Systems*, Cambridge University Press (1995), and Y. Imry, *Introduction to Mesoscopic Physics*, Oxford University Press, Inc. **(1997)**

[219] G. Grüner, *Density Waves in Solids*, Frontiers in Physics 89, Addison-Wesley Publishing Company (Massachusetts, Menlo Park, Ney York, **1994**)

[220] M. Bockrath, D. Cobden, J. Liu, A. G. Rinzler, R. Smalley, L. Balents, P.L. McEuen, *Nature* **397**, 598 **(1999)**

[221] S. Latil, S. Roche, D. Mayou, J.C. Charlier, *Phys. Rev. Lett.* 92, 256805 **(2004)**

[222] M. Glerup *et al.*, *Chem. Phys. Lett.* **387**, 193 (2004)

[223] C. Ewels, M. Glerup, *J. Nanosc. Nanotech.* **5**, p. 1345 (2005).

[224] K. McGuire *et al.*, *Carbon* **43**, p. 219 (2005)

[225] S.Y. Kim *et al.*, *Chem. Phys. Lett.* **413**, p. 300 (2005).

[226] B. Wei, R. Spolenak, P. Kohler-Redlich, M. Ruhle, E. Arzt, *Appl. Phys. Lett.* 74, p. 3149 **(1999)**

[227] R. Czerw *et al.*, *Curr. Appl. Phys*. **2**, p. 473 (2002)

[228] V. Krstić *et al.*, to be published

[229] K. Xiao, Y. Liu, P. Hu, G.Yu, Y. Sun, D. Zhu, *J. Am. Chem. Soc.* 127, 8614 **(2005)**

[230] V. Krstić *et al.*, cond-mat/0601513, to be published

[231] P.G. Collins, K. Bradley, M. Ishigami, A. Zettl, *Science* 287 1801 **(2000)**

[232] O. Stephan, private communication **(2006).**